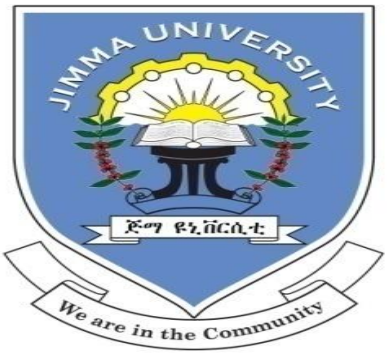

JIMMA UNIVERSITY

SCHOOL OF POST GRADUATE STUDIES

JIMMA INSTITUTE OF TECHNOLOGY

FACULTY OF CIVIL AND ENVIRONMETAL ENGINEERING

(Structural Engineering Stream)

Effect of Blast Loading On Seismically Detailed Reinforced Concrete Column Cross-Section

A thesis Submitted to the School of Graduate Studies of Jimma University in Partial Fulfillment of the Requirements for the Degree of Master of Science in Civil Engineering (Structural Engineering)

By

Lishan Beyene

May, 2018

Jimma, Ethiopia

JIMMA UNIVERSITY

SCHOOL OF POST GRADUATE STUDIES

JIMMA INSTITUTE OF TECHNOLOGY

FACULTY OF CIVIL AND ENVIRONMETAL ENGINEERING

(Structural Engineering Stream)

Effect of Blast Loading On Seismically Detailed Reinforced Concrete Column Cross-Section

A thesis Submitted to the School of Graduate Studies of Jimma University in Partial Fulfillment of the Requirements for the Degree of Master of Science in Civil Engineering (Structural Engineering)

By

Lishan Beyene

Main Advisor: Dr. Temesgen Wondimu (PhD)

Co-Advisor: Mr. Nataraj Palanisamy (Msc)

May, 2018

Jimma, Ethiopia

Declaration

I, the undersigned, declare that this thesis entitled "Effect of Blast Loading on Seismically Detailed Column Cross-Section" is my original work, and has not been presented by any other person for an award of a degree in this or any other University, and all sources of material used for these thesis have been duly acknowledged.

Lishan Beyene	_____	_____
Candidate	Signature	Date

As Master's Thesis Advisors, we here by certify that we have read and evaluated this MSc Thesis prepared under our guidance, by Lishan Beyene entitled: "Effect of Blast Loading on Seismically Detailed Column Cross-Section"

We recommend that it can be submitted as fulfilling the MSc Thesis requirements.

Dr. Temesgen Wondimu	_____	_____
Advisor	Signature	Date
Mr. Nataraj Palanisamy (MSc.).	_____	_____
Co- Advisor	Signature	Date

Acknowledgments

I would like to express my sincere gratitude to my main advisor, Dr. Temesgen Wondimu and Co. Advisor Mr. Nataraj Palanisamy for their continuous support together with their motivation and excellent guidance to carry out my work successfully. I would also like to thank my cousin Assistant Professor Bitiya Admassu for her valuable advices, useful suggestions and professional guidance given during the entire period of this study.

Last but not the least I would like to thank my parents, who taught me the value of hard work by their own example and for being there whenever I needed their support. I wish also to gratitude to my colleagues at JIT for sharing knowledge and encouragement at friendly and fruitful atmosphere. Finally, I am thankful to all those who have helped me in many ways to my successes.

Abstract

The vital need for the development of structural system that can survive the extreme events such as a blast load is becoming important nowadays. To date, the field of blast resistance design applied to civilian facilities is on its rudimentary stage. The conventional structures, particularly those above ground level, are not designed to resist blast load in most cases. Apparently, the design load of above ground structures are significantly lower than those produced by most explosions, making such above ground structures susceptible to damage from explosions. These facts are the main deriving forces for this thesis.

The response of different column cross-sections and column lengths subjected to lateral blast loads is examined. Rectangular and circular cross-sections are used in both short and slender type for the study. Short rectangular column is further studied with different transverse reinforcement spacing and scaled distance subjected to combined blast and axial loading. The finite element package Abaqus is used to model RC column with the same boundary conditions.

Short rectangular column is found to have better resistance than the others. Also short circular column has smaller lateral deflection than slender circular column. The result of the numerical study shows that the lateral reinforcement detailing has a significant effect on the behavior of columns under blast loading. Reducing the lateral reinforcement by 1/3 do not alter the result much but reducing by half the lateral reinforcement will reduce the lateral deflection significantly.

The effect of axial loading is also investigated in the numerical study. As the axial load ratio increases, the blast resistance of the concrete columns increased. However, at high axial load ratios, the lateral resistance is more of the same.

Key words: blast load, rcc, numerical modelling, wave propagation, dynamic response, axial load, time history analysis.

Table of Content

List of Tables

List of Figures

Acronyms

A_{ch}	Cross-sectional area of concrete core
A_g	Gross area of section
A_{st}	Total area of longitudinal steel
ALR	Axial Load Ratio
C3D8	8 node brick element
DIF	Dynamic Increase Factor
$\dot{\varepsilon}$	Strain rate
f_{cd}	Dynamic compressive strength
f_{ck}	Compressive strength of concrete
f_{cr}	Static compressive Strength
f_{yd}	Yield strength of steel
F_e	Equivalent load
FEM	Finite Element Method
i_r	Reflected impulse
K_e	Equivalent stiffness
KE	Equivalent stiffness factor
K_L	Load transformation factor
K_{LM}	Load mass factor
K_M	Mass transformation factor
M_e	Equivalent mass
ρ_c	Density of concrete
P_r	Reflected overpressure
P_{so}	Incident overpressure
P_{ult}	Factored axial load capacity
R	Standoff distance
r_u	Ultimate resistance
RC	Reinforced Concrete

SDOF	Single degrees of Freedom
t_a	Time of arrival
t_d^+	Positive phase duration
t_d^-	Negative phase duration
TNT	Trinitrotoluene
V_c	Volume of Column
Z	Scaled distance
W	Charge mass

Chapter One: Introduction

1.1. Background

In the past few decades considerable emphasis has been given to problems of blast loads and earthquake action. The problem of earthquake action is old and profound knowledge on the subject matter has been recorded well. In contrast, a blast problem is relatively new phenomena to civilian building structures. Moreover, scientific information about the development in blast loading field is made available mostly through publication of few organization like army corps of engineers, department of defense, and other governmental office and public institutes**.** Bomb explosions close to a building may cause casualties from direct overpressure of the blast, followed by falling of failed structural elements such as beams, column or slab. These explosions can also cause millions of dollars of property damage(1).

Bomb explosions in buildings have occurred relatively more frequently around the world in recent decades. A short survey of these explosions follows. Terrorists exploded a bomb in the 110 storey World Trade Centre in New York City in February 1993. The bomb was placed in an underground car park two storeys below ground level, causing major damage to the basement level of the building.

The bombing of the Alfred P. Murrah Federal Building in Oklahoma City, in April 1995 was the result of a truck bomb containing 1800kg of TNT equivalent, located approximately 5m from the north face of the building. Severe damage occurred to the nine storey reinforced column and slab construction, together with 168 casualties and US$50 million damage. Most importantly, surveys after the event indicated that the progressive collapse was initiated by the loss of integrity of four columns which extended the damage beyond the direct blast effects. Similarly, the attack on the Twin Towers of the World Trade Centre in New York City, September 2001 was responsible for the death of 3000 people.

The number of bombing attacks on modern societies has increased dramatically in recent years calling structural engineers to consider explosion loading more seriously in their design and trying to secure methods of construction facilities that will survive blast loads due to explosions(2).Blast loading and its effects on a structure is influenced by a number of factors including charge weight (W), location of the blast (or standoff distance), geometrical configuration and orientation of the structure (or direction of the blast). Structural response will

differ according to the way these factors combine with each other. The potential threat of an explosion is random in nature. Therefore, the analysis becomes complex and it is necessary to identify the influence of each factor in relation to the most credible event when assessing the vulnerability of structures(3). Due to this reasons explosive loads and their effects on a building have attracted significant attention following these incidents. Planning and building control authorities now recognize the risks associated with such events in the present environment of global terrorism and have been introducing provisions in planning guidelines for mitigation of such impacts.

1.2. Statement of the Problem

The concerns of this thesis arise from the failure or damage of buildings and loss of lives in some of the terrorist attacks due to the fact that these buildings have been or are built without consideration of their vulnerability to such events.

Due to the increasing of terrorist's attacks by using explosives have made the design of blast resistant to conventional structures more significantly important in recent years in light of the increase in global terrorism. The failure of critical structural components, such as RC columns, can have devastating effects on the structure as a whole. RC columns are an integral part of the load carrying components (load path) in a building. Thus, it is found to be necessary to investigate the performance of load-bearing building members which are designed and detailed for other load types such as wind and earthquake when subjected to blast loading.

1.3. Objective

1.3.1. General Objective

The main objective of this research is to study the structural behavior of seismically detailed RC column cross-section subjected to blast loading.

1.3.2. Specific Objectives

- The development of finite element (Abaqus) model for studying the behavior of RC column subjected to blast loading.
- To study the effect of different column shape on the blast resistance of RC columns.
- To study the effect of axial loads on the blast resistance of RC columns.

- To investigate the effects of varying scaled distances of the explosive charges on the behavior of RC columns.

1.4. Significance of the study

Blast events have become a common occurrence in many cities today. Despite this, there is no guidance freely available to assess the vulnerability of buildings to a near field blast load rather information about the development in this field is made available mostly through publication of the Army Corps of Engineers, Department of Defense, U.S. Air Force and other governmental office and public institutes. Much of the work is done by the Massachusetts Institute of Technology, The University of Illinois, and other leading educational institutions and engineering firms.

Until this point in time there was limited individual research carried out in our country to identify the blast response of RC column followed by a rigorous analysis to evaluate the damage to this elements where blast pressure is directly applied. This research will help as a guidance for the future study in this field.

Chapter Two: Literature Review

2.1. General

An explosion is a rapid and sudden release of stored potential energy characterized by a bright flash and an audible blast. Part of the energy is released as thermal radiation (flash); and part is coupled into the air as air blast and into the soil (ground) as ground shock, both as radially expanding shock waves(4).

The analysis of the blast loading on the structure started in 1960's. US Department of the Army, released a technical manual titled "structures to resist the effects of accidental explosions" in 1969. The manual presents procedures for determining the blast effects resulting from an accidental explosion and also techniques for the design of reinforced concrete structures which will provide protection for personnel, equipment and other explosive items(5).

In conventional design, RC columns predominantly transmit gravity loads from top floors of the building to the foundations. The total or partial loss of capacity of an RC column results in the redistribution of loads to adjacent structural components. The redistributed loading can result in the overload of the adjacent structural components beyond their load carrying capacities and can lead to their partial or total collapse. The total or partial collapse of the column and the tributary beams and floors, referred to as progressive collapse, is a common failure phenomenon associated with structures subjected to blast loading(2,3). Thus, the preventative design principles against progressive collapse is to ensure RC columns are designed and detailed with adequate strength and ductility, especially at the lower stories.

2.2. Explosive and blast waves

2.2.1. Classification of Explosions

Explosions are classified into two major categorizes. External explosions, blasts in an open environment, and Internal explosions, blasts inside a covered container or building. Further classification is made depending on the confinement of an explosive charge: Unconfined, Confined and Explosive attached to a structure. Table 2.1 shows an overview of possible loading categories(6).

Table 2.1 Possible Loading Categories(6).

Charge Confinement	Categories
Unconfined	The explosion in the free air
	The explosion in the air
	The explosion near the ground
Confined	Full ventilation
	Partially Confined
	Fully Confined

2.2.2. Blast wave phenomena

When an explosion occurs it will result in a production of exceedingly high temperatures and pressures due to the expanding hot gases that are created. The expansion leads to wave type propagation in the surrounding medium in a spherical form and a shock front or blast wave is produced as the hot gases compresses the surrounding air. The blast wave is instantly increased to higher pressure levels than the ambient atmospheric pressure. This high energy intensity decreases as the blast wave moves further away from the explosion source and may after a short time drop below ambient pressure before evening out, as demonstrated in Figure 2.1. This ideal pressure time history is illustrated in Figure 2.2 from Ngo et. als report on blast effects(1). As seen in this figure there are a portion above and a one below the ambient pressure value, P_o, of the pressure-time profile. These two portions is usually referred to as the positive phase of duration, t_d, and negative phase of duration, t_d^-.

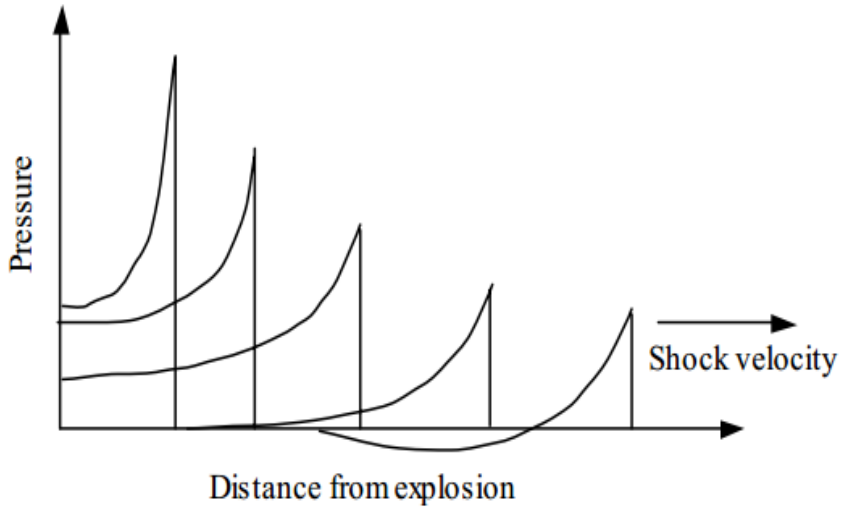

Figure 2.1. Propagation of overpressure with distance(5).

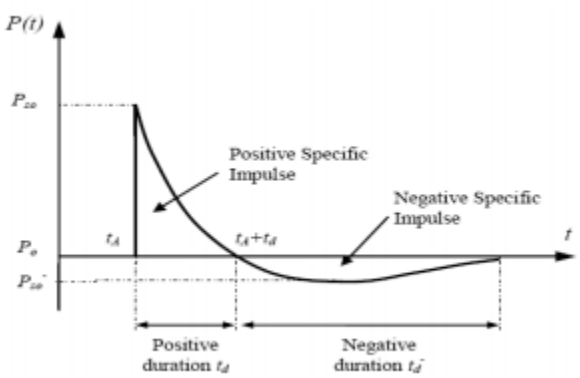

Figure 2.2. Time history for Blast wave pressure(5).

2.2.3. Stand-off distance and charge weight

The two most relevant variables that are crucial when mentioning threats from a conventional bomb are the charge weight W, and the stand-off distance R, between the detonation and the target, as seen in Figure 2.1. As Ngo et al(1) mentioned, the range of explosive attacks from terrorist varies from a small letter bomb to a large truck bomb as used in the Oklahoma City bombing. Table 2.2 shows some estimates of the quantity of explosives that could be transported in different sets of vehicles.

Table 2.2 Upper limits of charge weight per means of transportation

Carrier	Explosive Weight (kg)
Suitcase	10
Medium Car	200
Large Car	300
Pick-up truck	1400
Van	3000
Truck	5000
Truck with trailer	10000

2.2.4. Blast waves Scaling Laws

All blast parameters are primarily dependent on the amount of energy released by a detonation in the form of a blast wave and the distance from the explosion. For convenience, however, it is general practice to express the basic explosive input or charge weight as an equivalent mass of TNT(1).

The Hopkinson-Cranz scaling law or the cube-root scaling law is based on the notion that the detonation of an explosive of a particular charge weight, W_1, at a set stand-off distance, R_1, from a target will produce blast wave parameters such that the incident pressure, blast duration and impulse, will be similar to the blast wave parameters produced by another charge weight, W_2, at a corresponding scaled distance, R_2, detonated in the same atmospheric conditions. Results are then given as a function of the dimensional distance parameter, (7).

$$\frac{R_1}{R_2} = \left(\frac{W_1}{W_2}\right)^{1/3}$$

$$\text{Scaled Distance}\,(Z) = \frac{R}{W^{1/3}} \qquad [2.1]$$

Where R is the actual effective distance from the explosion

W is generally expressed in kilograms.

Scaling laws provide parametric correlations between a particular explosion and a standard charge of the same substance.(1)

2.2.5. TNT Equivalence

Different explosive materials release different amounts of energy per unit mass (energy density) upon detonation. The nature of the shockwave produced and the magnitude of the pressure generated from an explosion is thus dependent on the type of explosive involved. This creates a potential difficulty in blast load analysis as various explosive materials generate unique blast wave parameters in an explosion and would require knowledge of explosion behavior and characteristics of a large number of explosives(8,9). Trinitrotoluene (TNT) is, therefore, used as the standard explosive to which all other explosives are compared and their equivalence to TNT established. TNT equivalence is used to represent the mass of TNT that will produce the same amount of energy or explosion effects as a unit mass of a particular explosive in an explosion(10). TNT conversion factors have been determined for different explosive materials and tabulated in a number of blast design guides(11).

2.2.6. Prediction of Blast Pressure

There are various relationships and approaches for determining the incident pressure value at a specific distance from an explosion. All the proposed relationships entail computation of the scaled distance, which depends on the explosive mass and the actual distance from the center of the spherical explosion.

The estimations of peak overpressure due to spherical blast based on scaled distance $Z = R/W^{\frac{1}{3}}$ were introduced by Brode (1955), as shown in equations [2.2]. They depend on the magnitude of the explosion, Equation [2.2a] is valid where the peak overpressure is over 10bar (=1MPa) (near field explosions) and Equation [2.2b] for pressure values between 0.1 bar and 10 bar (0.01MPa-1MPa) (medium and far-field explosions). The scaled distance is measured in $m/kg^{1/3}$ and the pressure P_{so} in bars,

$$P_{so} = 6.7/Z^3 + 1bar \qquad (P_{so} \succ 10bar) \qquad [2.2a]$$

$$P_{so} = 0.975/Z + 1.455/Z^2 + 5.85/Z^3 - 0.019bar \qquad (0.1 \prec P_{so} \prec 10bar) \qquad [2.2b]$$

In 1961, Newmark and Hansen introduced a relationship to calculate the maximum blast overpressure, P_{so} in bars, for a high explosive charge detonates at the ground surface as:

$$P_{so} = 6784 W/R^3 + 93\left(W/R^3\right)^{1/2} \qquad [2.3]$$

In 1985, Kinney and Graham presented a formulation that is based on chemical type explosions. It is described by Equation [2.4] and has been used extensively for computer calculation purposes,

$$P_{so} = P_o \frac{808\left[1+\left(\frac{Z}{4.5}\right)^2\right]}{\left\{\left[1+\left(\frac{Z}{0.048}\right)^2\right]\left[1+\left(\frac{Z}{0.32}\right)^2\right]\left[1+\left(\frac{Z}{1.35}\right)^2\right]\right\}^{0.5}} \qquad [2.4]$$

Where $Z(m/kg^{1/3})$ is the scaled distance and P_o is the ambient pressure.

In 1987, Mills also introduced expression of the peak overpressure in kpa, in which W is the equivalent charge weight in kg of TNT and Z is the scaled distance.

$$P_{so} = 1772/Z^3 - 114/Z^2 + 108/Z \qquad [2.5]$$

As the blast wave propagates through the atmosphere, the air behind the shock front is moving outward at lower velocity. The velocity of the air particles, and hence the wind pressure, depends on the peak overpressure of the blast wave. This later velocity of the air is associated with the dynamic pressure, $q(t)$. The maximum value, $q(s)$, say, is given by

$$q(s) = \frac{5P_{so}^{\ 2}}{2(P_{so} + 7P_0)} \qquad [2.6]$$

If the blast wave encounters an obstacle perpendicular to the direction of propagation, reflection increases the overpressure to a maximum reflected pressure P_r as:

$$P_r = 2P_{so}\left\{\frac{7P_0 + 4P_{so}}{7P_o + P_{so}}\right\} \qquad [2.7]$$

A full discussion and extensive charts for predicting blast pressures and blast durations are given by Mays and Smith (1995) and TM5-1300 (1990). Some representative numerical values of peak reflected overpressure are given in Table 2.3.

Table 2.3 Peak reflected overpressure P_r (in MPa) with different W-R combinations(1).

W / R	100kg TNT	500kg TNT	1000kg TNT	2000kg TNT
1m	165.8	354.5	464.5	602.9
2.5m	34.2	89.4	130.8	188.4
5m	6.65	24.8	39.5	60.19
10m	0.85	4.25	8.15	14.7
15m	0.27	1.25	2.53	5.01
20m	0.14	0.54	1.06	2.13
25m	0.09	0.29	0.55	1.08
30m	0.06	0.19	0.33	0.63

For design purposes, reflected overpressure can be idealized by an equivalent triangular pulse of maximum peak pressure P_r and time duration t_d, which yields the reflected impulse (i_r).

$$i_r = \frac{1}{2} P_r t_d \qquad [2.8]$$

2.3. Structural Response to Blast Loading

Complexity in analyzing the dynamic response of blast-loaded structures involves the effect of high strain rates, the non-linear inelastic material behavior, the uncertainties of blast load calculations and the time-dependent deformations. Therefore, to simplify the analysis, a number of assumptions related to the response of structures and the loads has been proposed and widely accepted. To establish the principles of this analysis, the structure is idealized as a single degree of freedom (SDOF) system and the link between the positive duration of the blast load and the natural period of vibration of the structure is established. This leads to blast load idealization and simplifies the classification of the blast loading regimes(1).

2.3.1. Elastic Single Degrees of freedom (SDOF) system

To approximate the dynamic response of the column to the blast loads, the complex characteristics are simplified to an equivalent SDOF system. As the parameter of greatest interest is the displacement at the center (mid-point) of the column, all equivalent parameters are referenced to this point, with the displacement of the equivalent system equal to the mid-point displacement of the actual column(12).

The equation of motion for such a system resulted in a linear, second-order ordinary differential equation with constant coefficients, namely,

$$m\ddot{y} + c\dot{y} + ky = F(t) \qquad [2.9]$$

The blast load can also be idealized as a triangular pulse having a peak force F_o and positive phase duration t_d see figure 2.3.

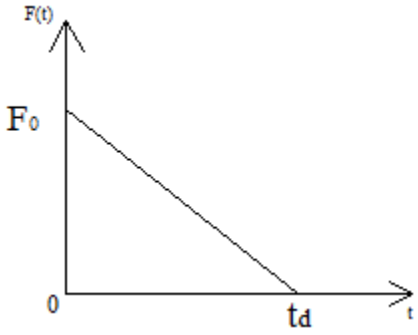

Figure 2.3: Idealized triangular blast load function(12).

The forcing function is given as

$$F(t) = F_o\left(1 - \frac{t}{t_d}\right) \qquad [2.10]$$

The blast impulse is approximated as the area under the force-time curve, and is given by

$$I = \frac{1}{2} F_o t_d \qquad [2.11]$$

2.3.2. Elasto-plastic Single Degrees of Freedom (SDOF) system

Structural elements are expected to undergo large inelastic deformation under blast load or high velocity impact. Exact analysis of dynamic response is then only possible by step-by-step numerical solution requiring a nonlinear dynamic finite-element software. However, the degree of uncertainty in both the determination of the loading and the interpretation of acceptability of the resulting deformation is such that solution of a postulated equivalent ideal elasto-plastic SDOF system is commonly used(12).

Interpretation is based on the required ductility factor $\mu = y_m / y_e$

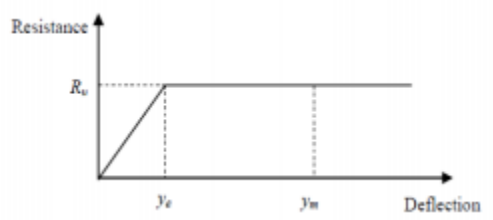

Figure 2.4 Simplified resistance function of an elasto-plastic SDOF system(1).

2.4. Strain Rate Effects

When a structural element is subjected to blast loading, strain rates typically vary in the range of $10^2 - 10^4\, s^{-1}$. For reinforced concrete structures subjected to blast effects the strength of concrete and steel reinforcing bars can increase significantly due to strain rate effects. This strength enhancement is represented by the "*dynamic increased factor*" (*DIF*) in the blast analysis and is discussed in terms of changing strain rate. Figure 2.5 shows the approximate ranges of the expected strain rates for different loading conditions. It can be seen that ordinary static strain rate is located in the range of $10^{-6} - 10^{-5}\, s^{-1}$, while blast pressures normally yield loads associated with strain rates in the range of $10^2 - 10^4\, s^{-1}$ (13).

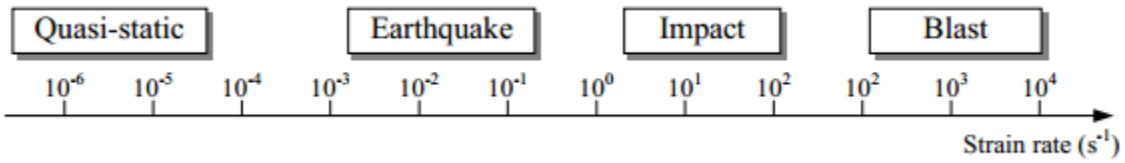

Figure 2.5 Strain rates associated with different types of loading(1).

Strength magnification factors as high as 4 in compression and up to 6 in tension for strain rates in the range of $10^2 - 10^3$ / sec have been reported (Grote et al., 2001)(14). The variation of the stress-strain relationship with strain rate is presented in Figure 2.6 for grade 40 concrete.

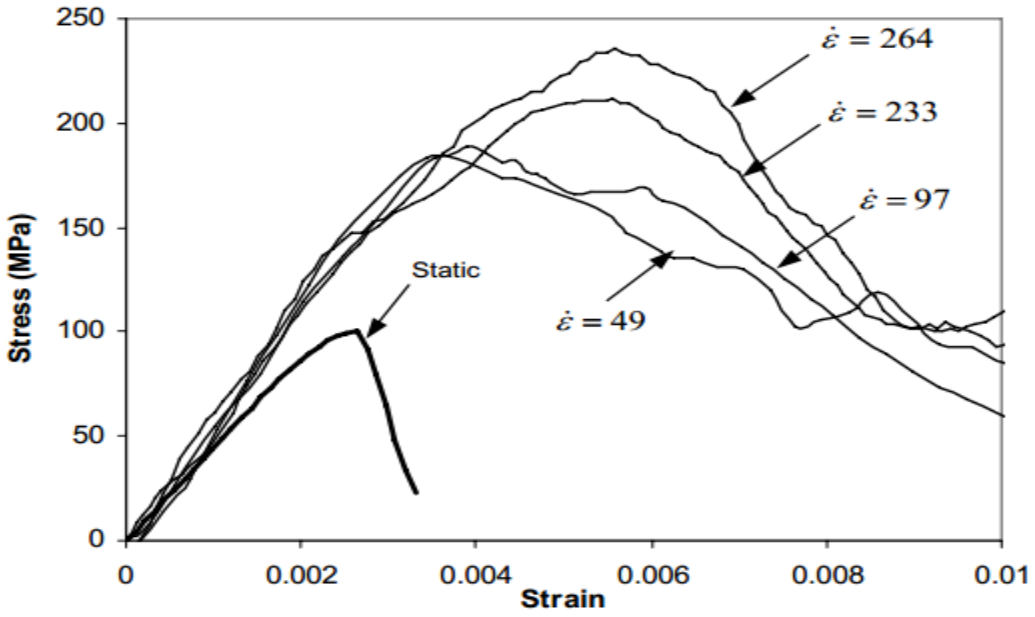

Figure 2.6 Stress strain curves of concrete at different strain rates

For compressive strength, CEB (1993) writes that the ratio of dynamic to static strength (DIF) is(13).

$$DIF = \frac{f_{cd}}{f_{cs}} = \left\{ \frac{\dot{\varepsilon}}{\dot{\varepsilon}_s} \right\}^{1.026\alpha} \qquad \text{for } \dot{\varepsilon} \le 30 s^{-1} \qquad [2.12]$$

$$DIF = \gamma \left\{ \frac{\dot{\varepsilon}}{\dot{\varepsilon}_s} \right\}^{0.33} \qquad \text{for } \dot{\varepsilon} \succ 30 s^{-1} \qquad [2.13]$$

Where f_{cd} is the dynamic compressive strength at strain rate $\dot{\varepsilon}$ in the range of $30 \times 10^{-6} s^{-1}$ to $300 s^{-1}$, f_{cs} is the static compressive strength at a reference strain rate $\dot{\varepsilon}_s$ of $30 \times 10^{-6} s^{-1}$, $\log \gamma = 6.156\alpha - 2$ $\alpha = 1/(5 + 9 f_{cs} / f_{co})$ and $f_{co} = 10MPa$.

For strength enhancement of steel reinforcing bars under the effect of high strain rates was described in terms of the dynamic increase factor (DIF), which can be evaluated for different steel grades and for yield stresses, f_y, ranging from 290 to 710MPa as represented by equation [2.14].

$$DIF = \left\{ \frac{\dot{\varepsilon}}{10^{-4}} \right\}^{\alpha} \qquad [2.14]$$

Where for calculating yield stress $\alpha = \alpha_{fy}$

$$\alpha_{fy} = 0.074 - 0.04(f_y / 414) \qquad [2.15]$$

For ultimate stress calculation $\alpha = \alpha_{fy}$

$$\alpha_{fy} = 0.019 - 0.009(f_y / 414) \qquad [2.16]$$

2.5. Nonlinearity in Reinforced Concrete

The nonlinearities in reinforced concrete members can be geometric as well as material. Both of these become very important at higher level of deformations.

2.5.1. Geometric nonlinearity

Geometric nonlinearity is related to changes in the geometry of the structure during the analysis. Geometric nonlinearity occurs whenever the magnitude of the displacements affects the response of the structure. This may be caused by:

- Large deflections or rotations.
- "Snap through."
- Initial stresses or load stiffening.

Incorporating the effects of geometric nonlinearity in an analysis requires only minor changes to an Abaqus/Standard model. In Abaqus/Explicit geometric nonlinearity is a default setting. So select Abaqus/Explicit in Step definition.

2.5.2. Material Nonlinearity

Concrete and steel are two constituents of R.C.C. Steels have a fairly linear stress/strain relationship at low strain values; but at higher strains the material yields, at which point the response becomes nonlinear and irreversible. While the tensile stress – strain relationship of concrete is almost linear; the stress-strain relationship in compression is nonlinear from the beginning. Since the concrete and steel are both strongly nonlinear materials, the material nonlinearity of reinforced concrete is a complex combination of both.

Material nonlinearity may be related to factors other than strain. Strain-rate-dependent material data and material failure are both forms of material nonlinearity. Material properties can also be a function of temperature and other predefined fields.

In Abaqus each material definition is given a name. Different regions in a model are associated with different material definitions through the assignment of section properties that refer to the material name.

2.6. Stress-Strain curves of Concrete and Steel

2.6.1. Stress-Strain curves of Concrete

Many textbooks present stress-strain relationships for concrete in uniaxial compression. Sample relationships are presented in Figure 2.7 from Wight and MacGregor (2008)(15) for concrete with compressive strength (f_{ck}) ranging between 4500 psi (31 MPa) and 17500 psi (120 MPa). The curves are somewhat linear in the very initial phase of loading; the nonlinearity begins to gain significance when the stress level exceeds about one-third of the maximum. The maximum stress is reached at a strain approximately equal to 0.002; beyond this point, an increase in strain is accompanied by a decrease in stress. For the usual range of concrete strengths, the strain at failure is in the range of 0.003 to 0.005. The modulus of elasticity in units of psi for normal-weight concrete with a density of 145 lb/ft3 is often taken per ACI 318 as(13):

$$E_c = 57000\sqrt{f_{ck}} \qquad [2.17]$$

Where f_{ck} is in units of psi. Values of compressive strength are used to compute mechanical properties for design after modification for strain-rate effects.

A stress-strain relationship for normal-weight concrete in tension, which is reproduced in Figure 2.8. The tensile strength of concrete, (f_y), ranges between 8 and 15 percent of the compressive strength, with the value dependent on the type of test used for the measurement(13).

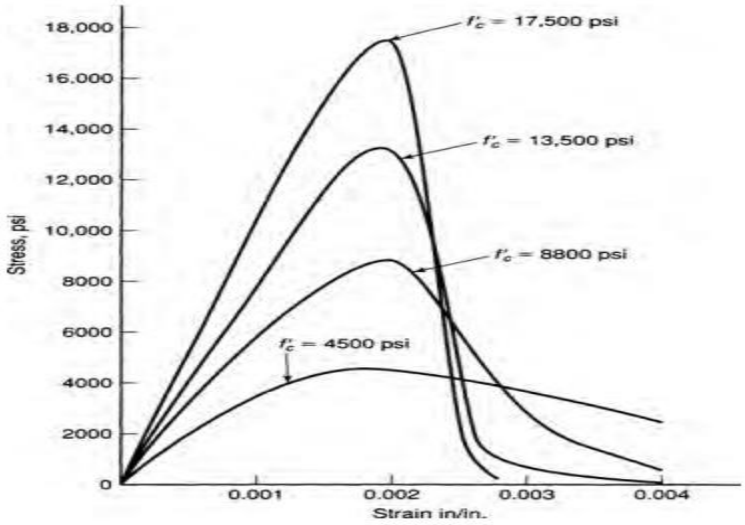

Figure 2.7: Stress-Strain Relationships for Concrete in Uniaxial Compression at Low Speed(13).

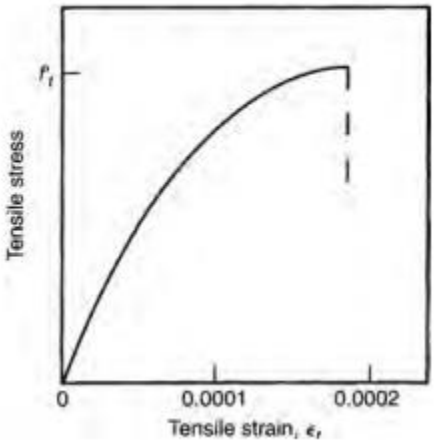

Figure 2.8: Generic Stress-Strain Relationship for Concrete in Tension(13).

2.6.2. Stress-Strain Curve of Steel

Typical stress-strain relationships for steel reinforcement (or rebar) are presented in standards and textbooks. Figure 2.9 presents a typical stress-strain relationship for Grade 60 rebar from Malvar (1998)(16). Generic uniaxial stress-strain relationships are also available for structural steels in textbooks and sample stress-strain relationships are presented in Figure 2.10. Steel,

when subjected to high stress levels, shows plasticity behavior, i.e. when all the forces acting on the body are removed, the body does not return its original shape, but has some permanent plastic deformation associated with it(13).

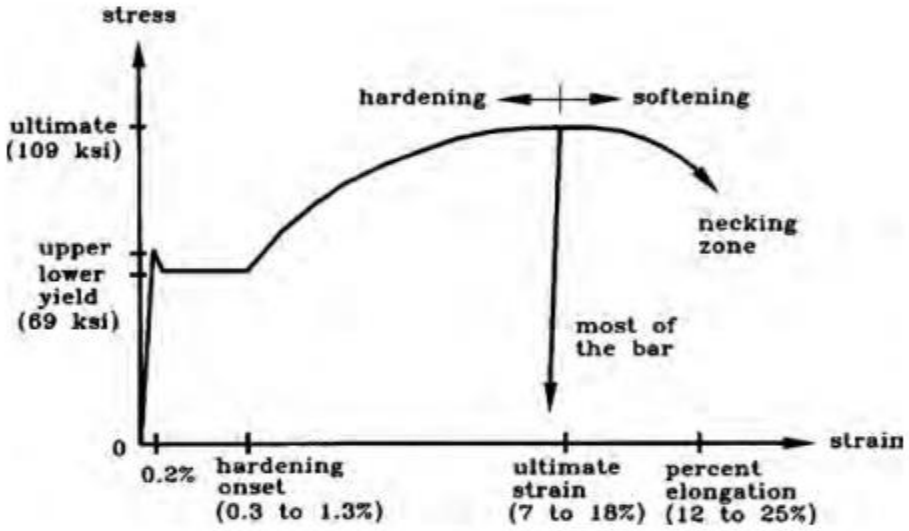

Figure 2.9: Typical Stress-Strain Relationship for Grade 60 Steel Reinforcement (8)

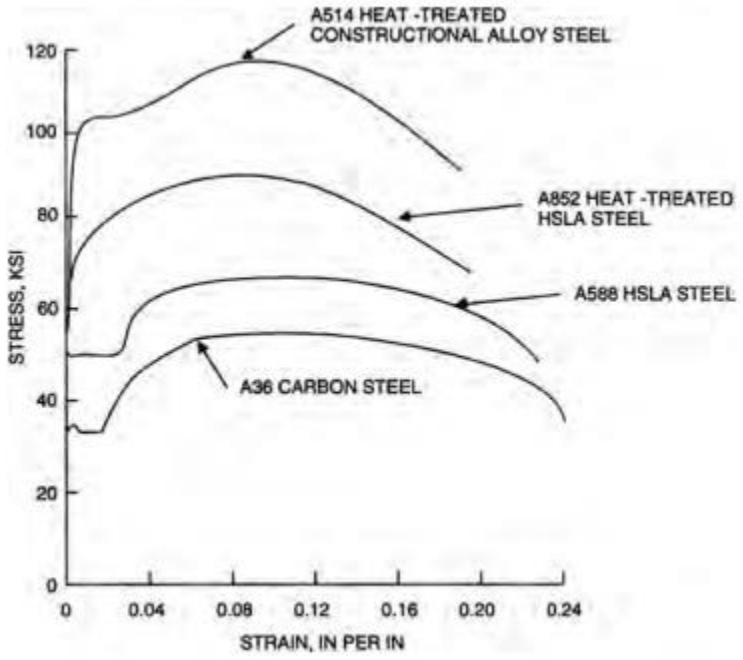

Figure 2.10: Stress-Strain Relationships for Selected Structural Steels (8)

Chapter Three: Methodology and Finite Element Analysis

3.1. Study Area

The RC columns under study are designed as Isolated Column for the same axial load and moments. The axil load and moments are taken from a Project on Building Codes of earthquake by *Dr. H. J. Shah* Department of Applied Mechanics, M. S. University of Baroda, Vadodara and *Dr. Sudhir K Jain* Department of Civil Engineering, Indian Institute of Technology Kanpur.

3.2. Study Design

The general purpose finite element software known as Abaqus is used to model and study the effects of blast loading on different RC column shapes. Prior to the comparison, the numerical model was validated with experimental results obtained from live explosion field tests.

3.3. Study Variables

The variables used in this study are dependent and independent Variables. Described as follows.

3.3.1. Dependent Variable

- The response of the Column

3.3.2. Independent Variable

- Cross-sectional shape of the column (Rectangular and Circular)
- Stand-off distance
- Charge mass
- Transverse reinforcement spacing
- Axial loading

3.4. Analysis

The analysis were done by using Abaqus computer simulation. Abaqus is a general purpose FEM program that can solve a variety of problems. Abaqus does not have any modules/ packages for machining simulations, and hence the user has to explicitly define the tool and work piece, the process parameters and the simulation controls (including boundary conditions and mesh geometry). Abaqus comes with two solvers (Standard and Explicit) which can be used to run a variety of simulations. Simulations are setup in Abaqus by using keywords that define the functioning of the simulation. Though Abaqus has no support for any materials, it allows users to configure the materials using a variety of models. The users also has very fine control over the

meshing and the element types used in the model. Perhaps the biggest advantage of Abaqus is that it allows modelling at a high level of detail. Due to this reasons Abaqus software was used for the analysis. The Abaqus result were first validated before comparison and parametric analysis.

3.5. Modelling Using Abaqus

Abaqus is general-purpose finite element software for numerically solving a wide variety of structural engineering problems. The Abaqus element library consists of many different types of elements. For the numerical simulation of any RC structure, three dimensional solid element C3D8 has been used for modeling the nonlinear behavior of concrete, three dimensional beam element has been used for modeling the reinforcement.

3.5.1. Solid Element (C3D8R)

Among the different element families, continuum or solid elements can be used to model the widest variety of components. Conceptually, continuum elements simply model small blocks of material in a component. Since they may be connected to other elements on any of their faces, continuum elements, like bricks in a building or tiles in a mosaic, can be used to build models of nearly any shape, subjected to nearly any loading. Abaqus/Explicit offers only linear elements. So in this thesis linear element is used. Typically, the number of nodes in an element is clearly identified in its name. This element is defined by eight nodes having three degrees of freedom at each node: translations in the nodal x, y, and z directions. The 8-node brick element, as you have seen, is called C3D8.

3.5.2. Beam Element

Beam element is a 3-dimensional spar (or truss) element. This element is used to model the steel in reinforced concrete. The three-dimensional spar element is a uniaxial tension-compression element with three degrees of freedom at each node: translations in the nodal x, y, and z directions. This element is also capable of plastic deformation.

3.6. Material Model

Material nonlinearity is considered in this thesis. The explicit dynamics procedure can be an effective tool for solving a wide variety of nonlinear solid and structural mechanics problems. Incorporating the effects of geometric nonlinearity in an analysis requires only minor changes to

an Abaqus/Standard model. You need to make sure the step definition considers geometrically nonlinear effects. This is the default setting in Abaqus/Explicit. However, depending upon the input given to the material models of concrete and steel in Abaqus, the response of the reinforced concrete column can be different. For the present analysis the following material models have been used.

3.6.1. Concrete

The model is a continuum, plasticity-based, damage model for concrete. It assumes that the main two failure mechanisms are tensile cracking and compressive crushing of the concrete material. This model assumes that the uniaxial tensile and compressive response of concrete is characterized by damaged plasticity, as shown in Figure 3.1.

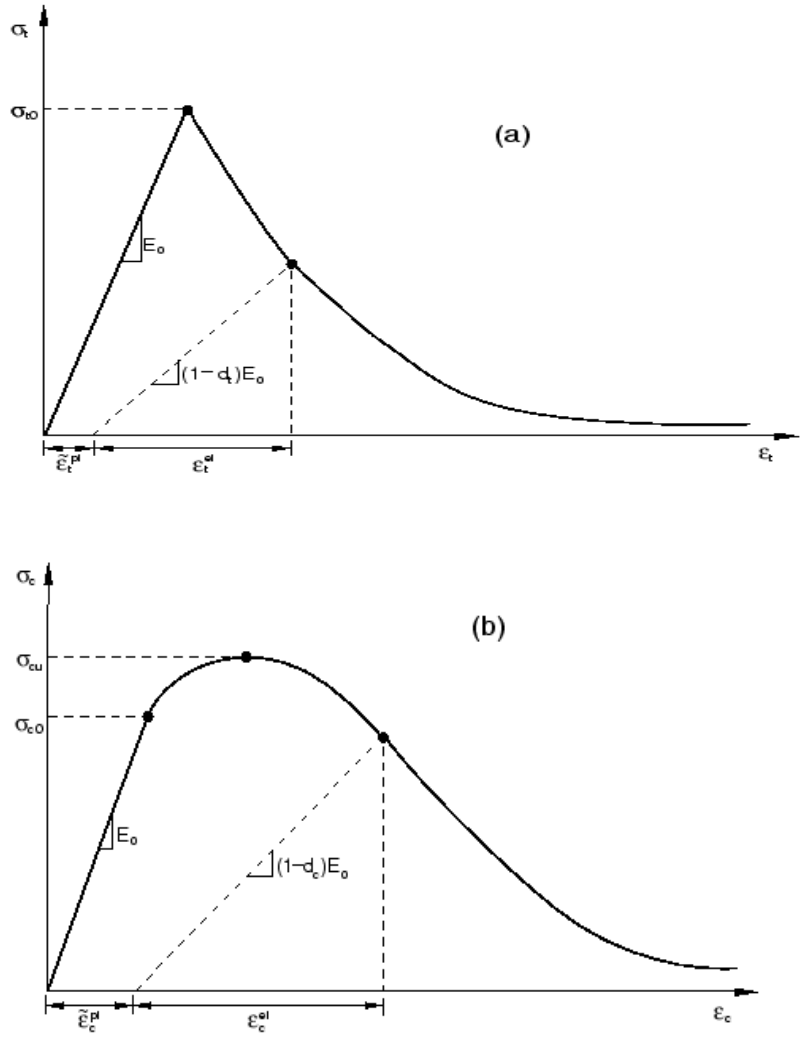

Figure 3.1: Response of concrete to uniaxial loading in tension (a) and compression (b).

Under uniaxial tension the stress-strain response follows a linear elastic relationship until the value of the failure stress is reached. Under uniaxial compression the response is linear until the value of initial yield. In the plastic regime the response is typically characterized by stress hardening followed by strain softening beyond the ultimate stress. This representation, although somewhat simplified, captures the main features of the response of concrete.

3.6.2. Reinforcing Bars

In Abaqus reinforcement in concrete structures is typically provided by means of rebar's, which are one-dimensional rods that can be defined singly or embedded in oriented surfaces. Rebar's are typically used with metal plasticity models to describe the behavior of the rebar material and are superposed on a mesh of standard element types used to model the concrete.

3.7. Bonding

With this modeling approach, the concrete behavior is considered independently of the rebar. In reinforced concrete, the concrete's weakness in tension is compensated for by the introduction of reinforcing bars. Effects associated with the rebar/concrete interface, such as bond slip and dowel action, are modeled approximately by introducing some "tension stiffening" into the concrete modeling to simulate load transfer across cracks through the rebar. Effective bonding of the plain concrete and the reinforcing bars ensures transmission of the tensile forces from the concrete to the reinforcing bar and eliminates the bond slip concern. In Abaqus simulations involving reinforced concrete, which involves separately meshing the concrete and reinforcement, effective bonding is achieved by embedding the reinforcement in concrete.

An element or a group of elements can be embedded in a group of host elements. ABAQUS will search for the geometric relationships between nodes on the embedded elements and the host elements. If a node on an embedded element lies within a host element, the degrees of freedom at the node will be eliminated by constraining them to the interpolated values of the degrees of freedom of the host element.

3.8. Loading

3.8.1. Blast Loading

The blast loading are read from the graph in Appendix A1 based on the calculated scaled distance. This loading is applied as pressure loads on the front face of the column. This loads are applied to the surface of the front face as linearly varying loads for a calculated blast time. Figure 3.2 (a) shows how the blast loading is applied in Abaqus on column.

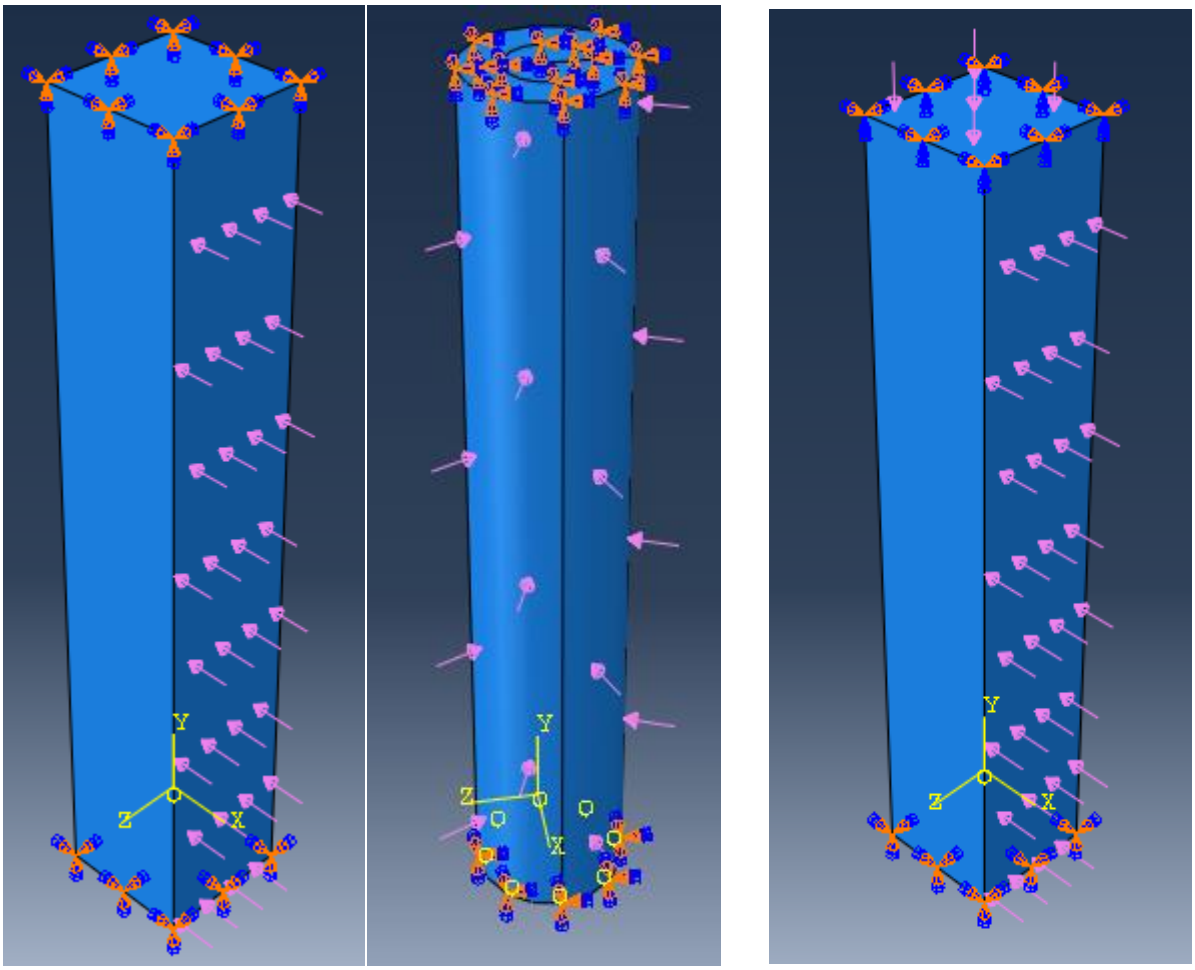

(a) Blast Loading (b) Combined blast & Axial Loading

Figure 3.2 (a) – (b) Loading used in Abaqus

3.8.2. Axial Loading

The axial loading is a representative of gravitational load from the higher story on the ground column. The axial loads corresponding to various axial load ratios (ALR) are applied as pressure loads on the top face of the column. The loads are applied to the surface of the top nodes as

uniformly distributed loads. To simulate the axial loading, the top node of Abaqus model were allowed to translate in the vertical direction in order to transmit the axial load (strains) see Figure 3.2 (b).

3.9. Description of the experimental data

For validation purpose one of the columns tested by Farouk (17)is taken. The selected column has a height of $3000mm$ and cross-section of $300mm \times 300mm$ reinforced with 4-25 mm diameter longitudinal bars with a concrete cover to reinforcement of 40mm. The 28-day concrete compressive strength is 41MPa while the yield strength of the steel was approximately 400MPa.

This column was designed and detailed for a building in a region of high seismicity and had 10 mm diameter transverse reinforcements spaced at 75mm over a plastic hinge length of 600mm close to the two supports. The transverse steel in the region between the plastic hinge lengths of the column was spaced at 150mm which was reduced to 75mm spacing in the mid-region.

The seismically detailed RC columns with the detailing scheme shown in Figure 3.4 was modelled and subjected to 84 kg of TNT (a TNT equivalent mass of the 100 kg of ANFO) used in experimental test program (Farouk 2013). The explosive was set at a stand-off distance of 2.5 m and a height of burst of 1 m.

The blast loading during the experiment used is converted to a pressure when applied on the Abaqus software by using the procedure indicated in appendix A.

- By applying 20% safety factor for the charge $W = 1.2 * 100kg = 120kg$
- Calculate Scaled distance

$$R = \sqrt{2.5^2 + 1^2} = 2.693m \qquad Z = \frac{R}{W^{1/3}} = \frac{2.693}{120kg^{1/3}} = 0.5$$

- Then Read the required values based on the calculated Z from Figure A1-b.

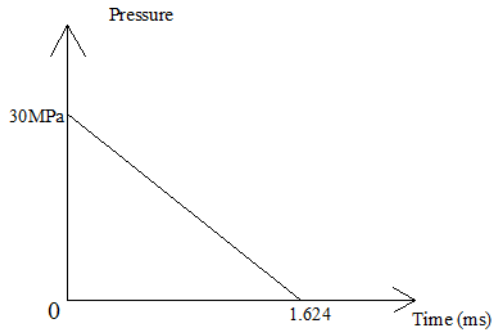

Figure 3.3 Equivalent blast function for experimental

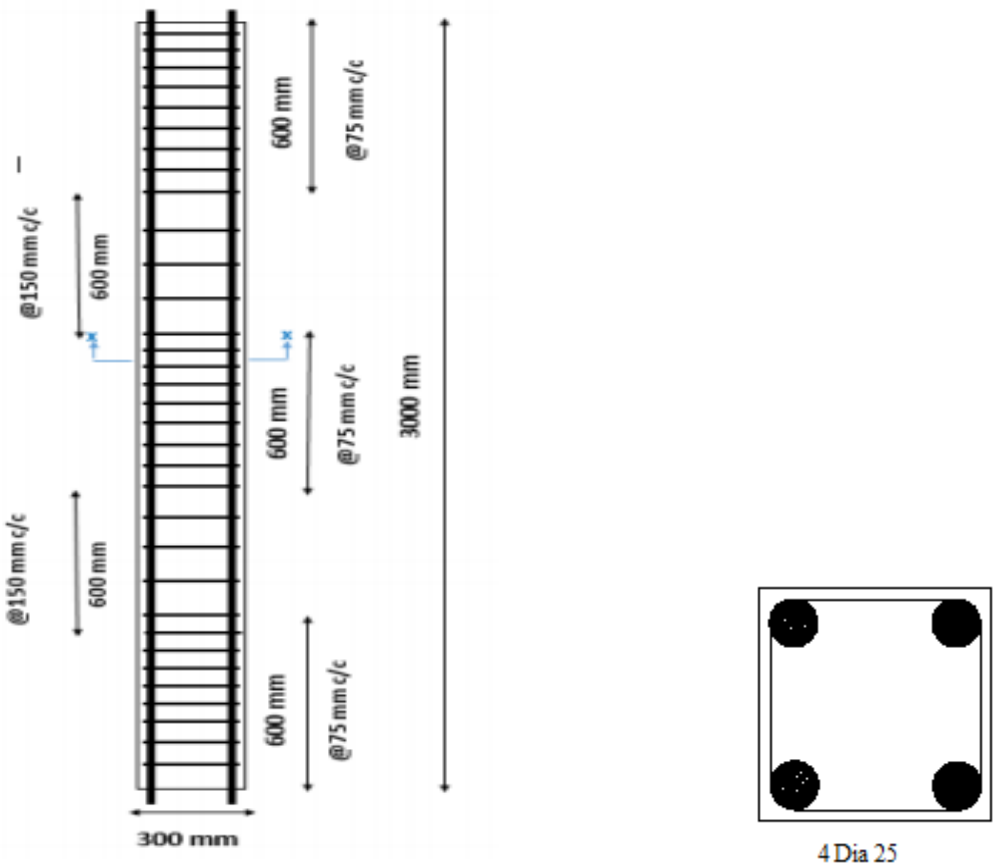

Figure 3.4 Reinforcement detailing for seismic column used in experimental work

The experimental results are modeled using finite element software ABAQUS, for validation, were meshed with approximate global size of 20mm. The modelled column was representative of the column and detailed in Figure 3.4. The nodes at the base and top of the column were all fixed to prevent translation as well as rotational movements in three cardinal directions.

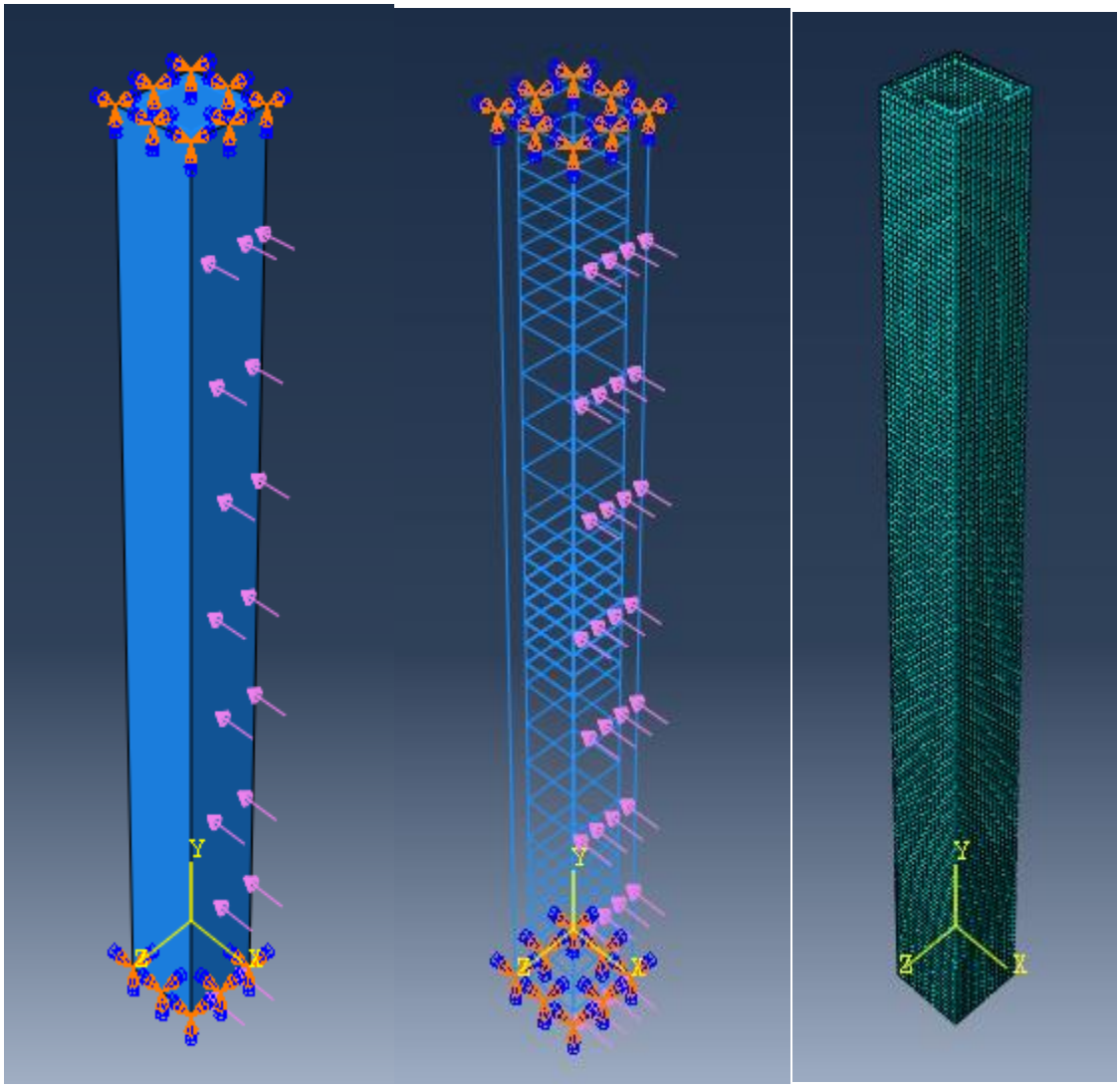

Figure 3.5 Abaqus modelling for the experimental

3.10. Single Degrees of Freedom Modeling

Effective Mass (M_e): -the effective mass is given by

$$M_e = V_c \times \rho_c \times k_{LM} \quad [3.1]$$

Where k_{LM} = Load mass factor, V_c = Volume of column, ρ_c = Density of concrete

Equivalent Stiffness (K_e)

The equivalent stiffness is also computed based on the support type and the load type. Table B2 gives the values of the KE based on the support and loading type.

$$K_e = KE \times L_c \quad [3.2]$$

Where KE = Equivalent stiffness factor

L_c = Length of column

Ultimate Resistance (r_u)

The ultimate resistance is given as a function of the maximum positive moment (M_P) and maximum negative moment (M_n) of resistance of the RC cross-section. The ultimate resistance values depending on the support and loading type are given in table B3.

Dynamic Increase Factors

The UFC writes that the values given in table 3.1 for flexure assume a strain rate of $0.02s^{-1}$ for both rebar and concrete in the low-pressure for reinforced concrete members in compression (i.e., columns).

Table 3.1: Dynamic increase factor for low pressure(13).

	Steel Reinforcement	Concrete
Flexure	1.17	1.19

Direct Shear	1.10	1.10
Diagonal Shear	1.00	1.00

Damping (C)

Damping is allowed into the equivalent SDOF model by incorporating a user-defined damping coefficient (ξ).

$$C = 2\sqrt{K_e M_e} \times \xi \qquad [3.3]$$

Blast Loading Function ($F(t)$)

The blast load can also be idealized as a triangular load pulse, initially at rest and subjected to a force $F(t)$ which has an initial value F_o and which decreases linearly to zero at time t_d. The response may be computed in two intervals(14).

The first interval for $0 \le t \le t_d$

$$F(t) = F_0\left(1 - \frac{t}{t_d}\right) \qquad [3.4]$$

The second interval for $t \succ t_d$

$F(t) = 0$

Chapter Four: Results and Discussion

4.1. Validation of ABAQUS model by Experimental Testing

The detailed scheme for the seismically detailed reinforced columns is shown in Figure 3.5. This representative columns for the experimental one is analyzed by Abaqus finite element software. This columns are analyzed by using different mesh size in order to select a better mesh size both in accuracy and reasonable time to complete the analysis.

Table 4.1 shows the maximum displacements from the different mesh size and number of elements associated with each mesh size. Table 4.1 also presents the maximum displacement recorded from the experimental work together deflections from the numerical simulations with the different mesh sizes. Depending on the result mess size 20mm was used for the comparison and parametric study.

Table 4.1 Mesh sensitivity analysis

Mesh Size (mm)	Number of Elements	Max. Displacement (mm)
50mm	2,236	46.35
30mm	10,128	34.19
20mm	33,944	34.12
Experimental		24.94

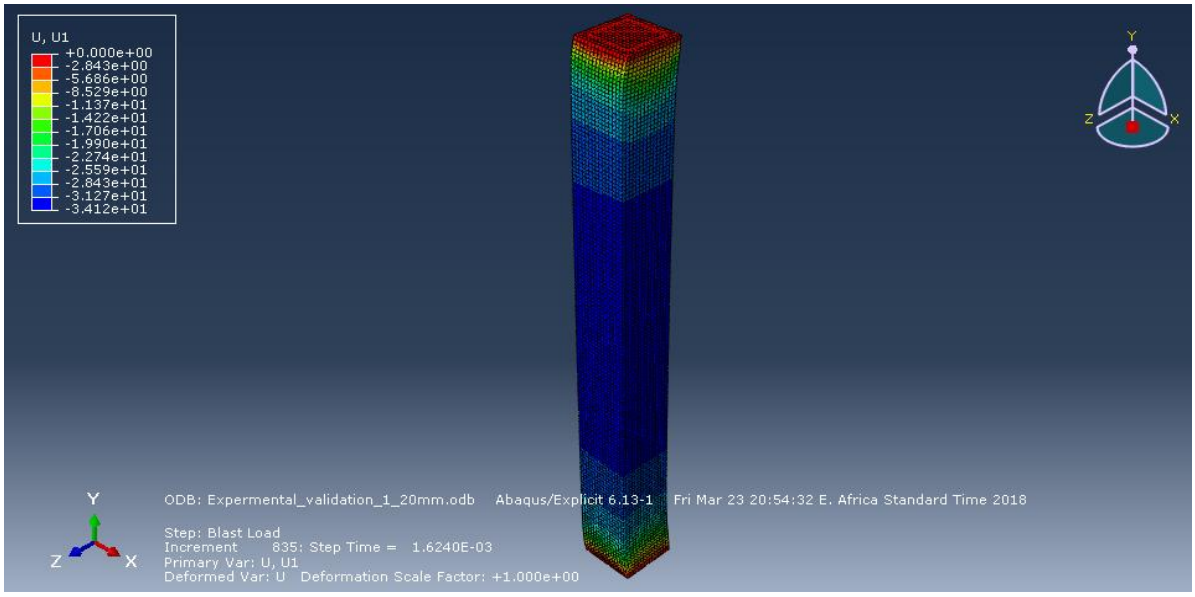

Figure 4.1: Result for representative experimental column from Abaqus software

4.2. Comparison between different RC column shapes

The first column type, designated as Short Rectangular, has a length of 3000mm and cross-section as shown in Figure 4.3a. The second RC column type, designation as Short Circular, has the same length as short rectangular but cross-section as shown in Figure 4.3c. The third RC column type, designation as Slender Rectangular, has a length of 4100mm and cross-section as shown in Figure 4.3b. The fourth RC column type, designation as Slender Circular, has the same length as slender rectangular but cross-section as shown in Figure 4.3d.

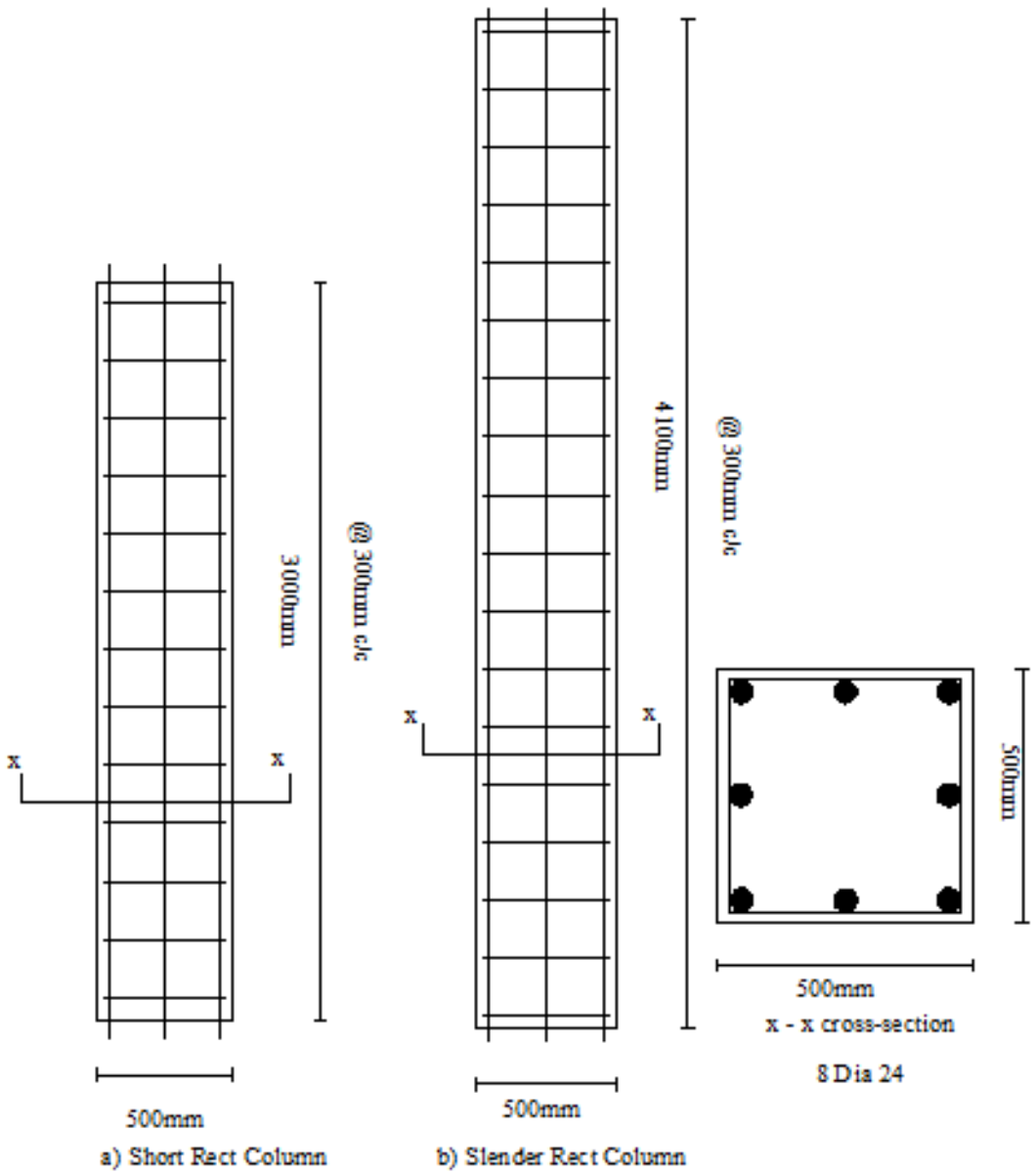
3000mm
@ 300mm c/c
x
x
500mm
a) Short Rect Column
4100mm
@ 300mm c/c
x
x
500mm
b) Slender Rect Column
500mm
500mm
x - x cross-section
8 Dia 24

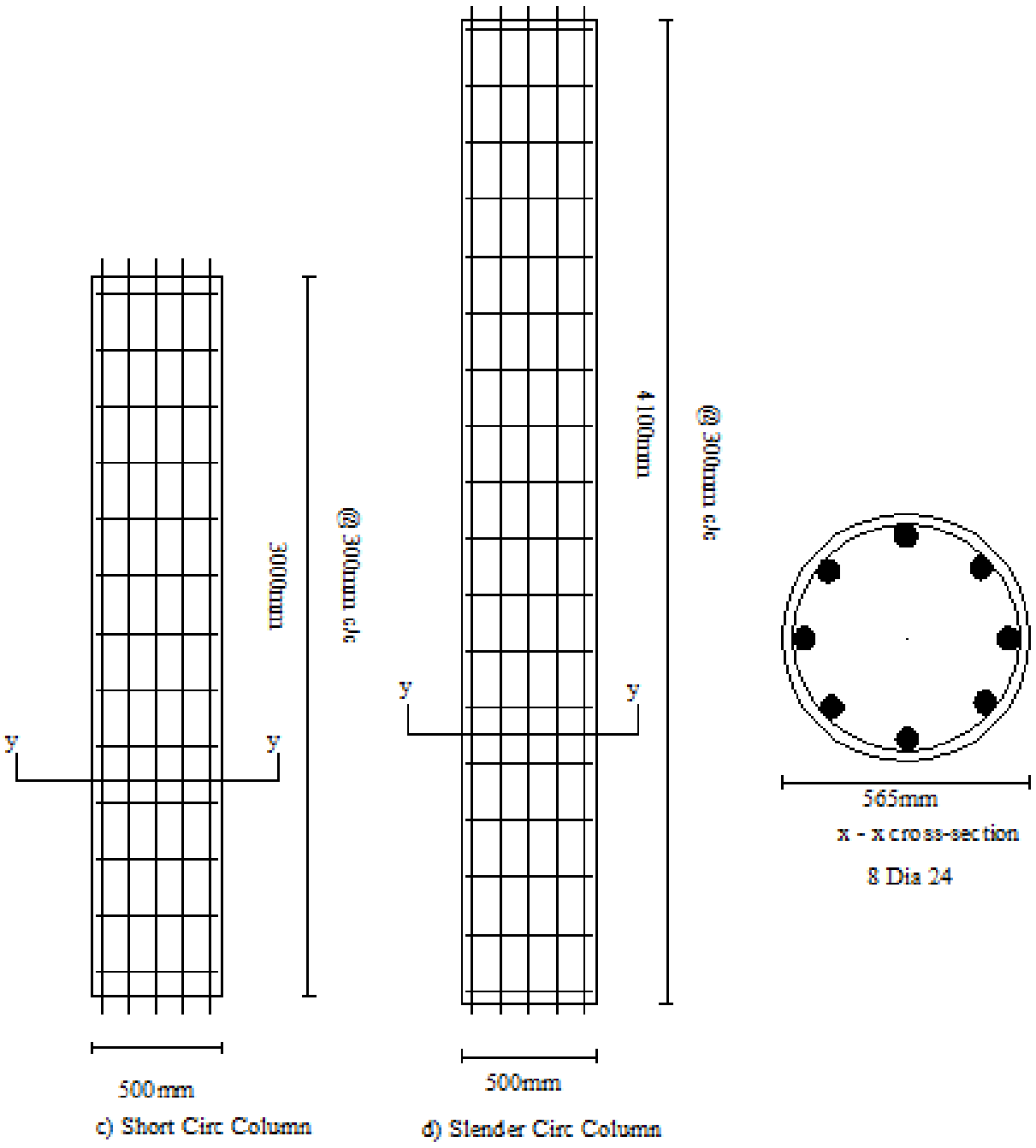

Figure 4.2: Column with different cross-section for the analysis

The Blast load is calculated for a charge mass of 250kg at a scaled distance of $1.0\,ft/lb^{1/3}$. The simplified triangle shape of the blast load profile was used as seen in Figure 4.3.

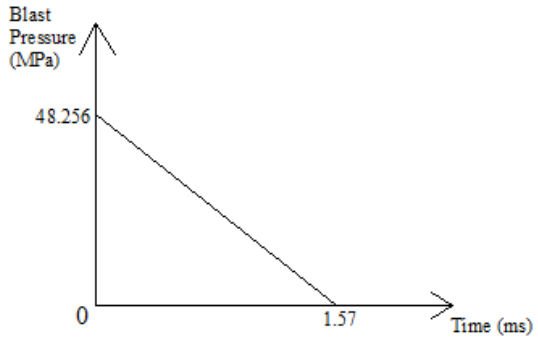

Figure 4.3: Blast Loading Function

The duration of the positive phase of the blast is 1.57 milliseconds. The 3D model of the column is analyzed using the Abaqus/Explicit which takes into account both material nonlinearity and geometric nonlinearity. The effects of the blast loading were modelled in the dynamic analysis to obtain the deflection time history of the column.

The lateral deflection at mid-point versus time history of four columns are shown in Figure 4.4. The graph clearly shows the lateral resistance of the columns. Short rectangular columns has produced 32.839mm maximum deflection which 10.56% reduced compared to short circular column 36.715mm.

Short rectangular column has produced 16.25% smaller lateral deflection compared to slender rectangular column with short column length to slender column length ratio of 0.732m. Whereas short circular column has produced 13.39% smaller lateral deflection compared to the slender circular with the same ratio as rectangular.

Generally, short columns in both cross-sections (rectangular and circular) have better resistance in comparison to the slender columns and also the rectangular cross-section will have better resistance to that of circular cross-section. This shows that short rectangular column is better in resistance.

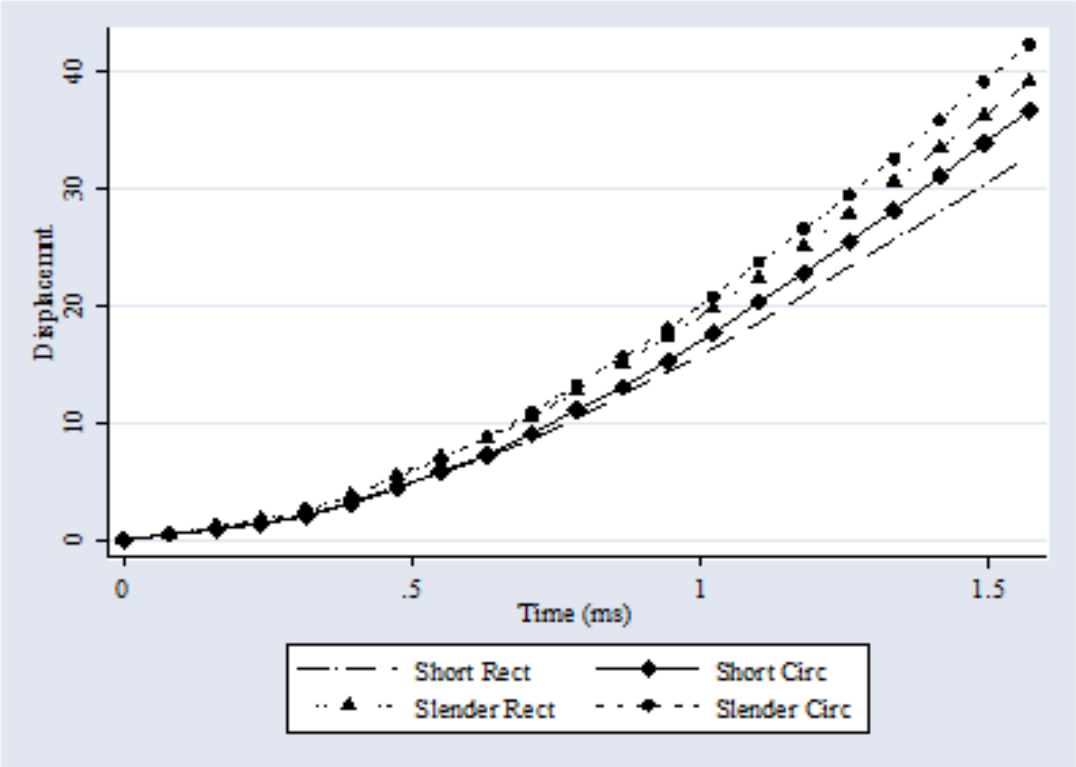

Figure 4.4: Displacement time history for the different cross-sectional columns

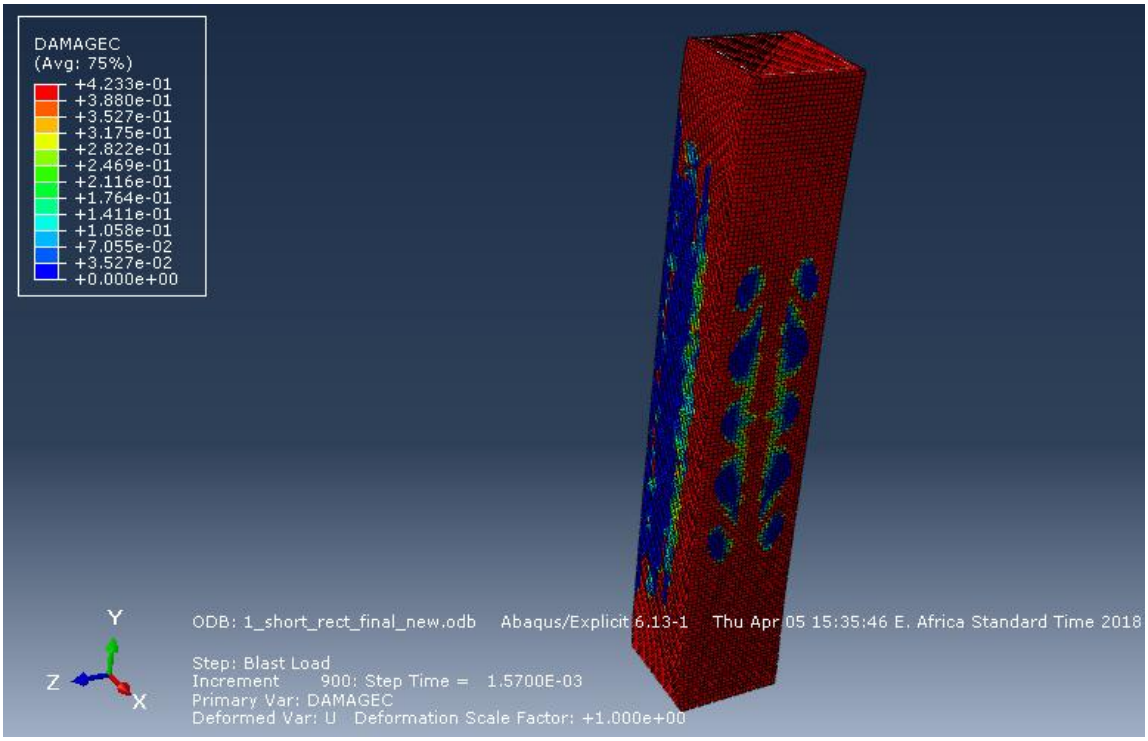

(a) Short rectangular column DamageC

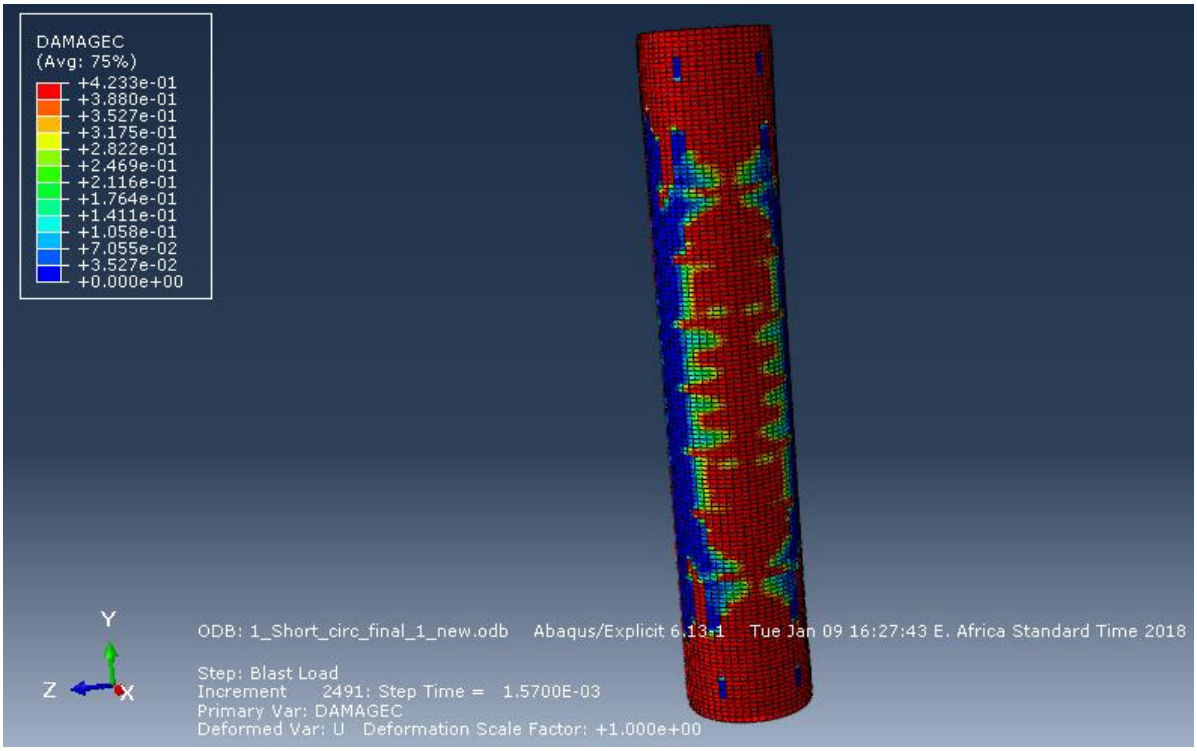

(b) Short Circular column DamageC

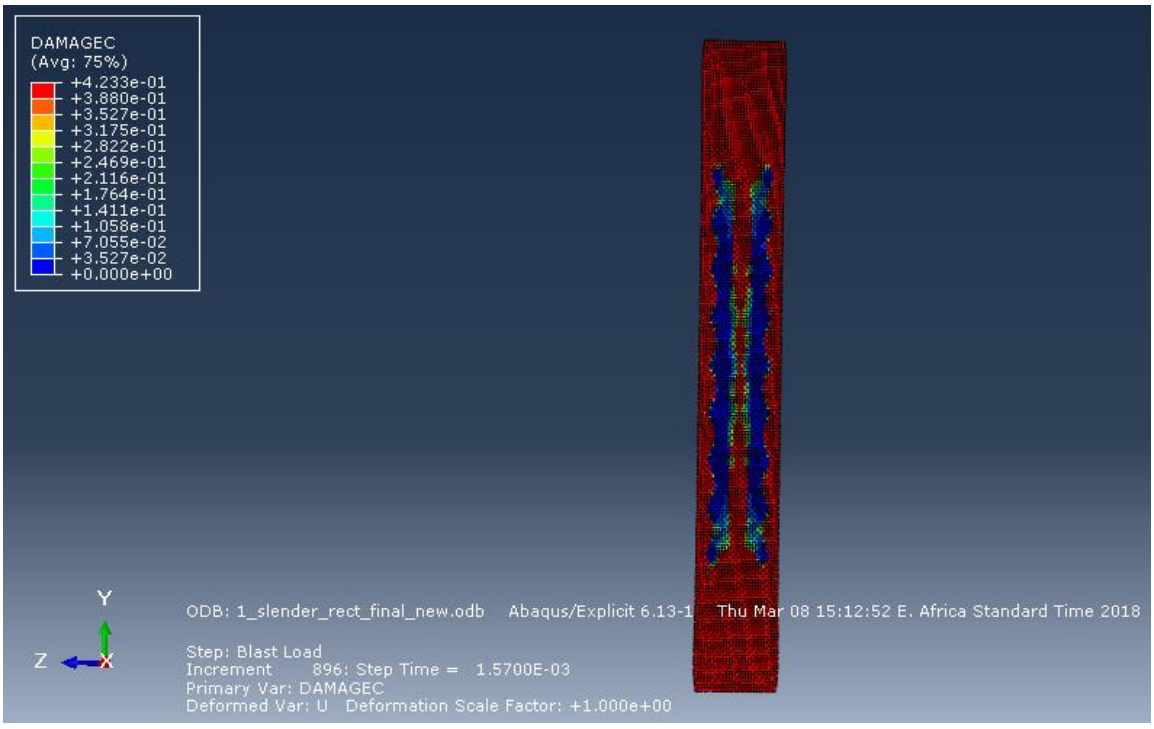

(c) Slender rectangular column DamageC

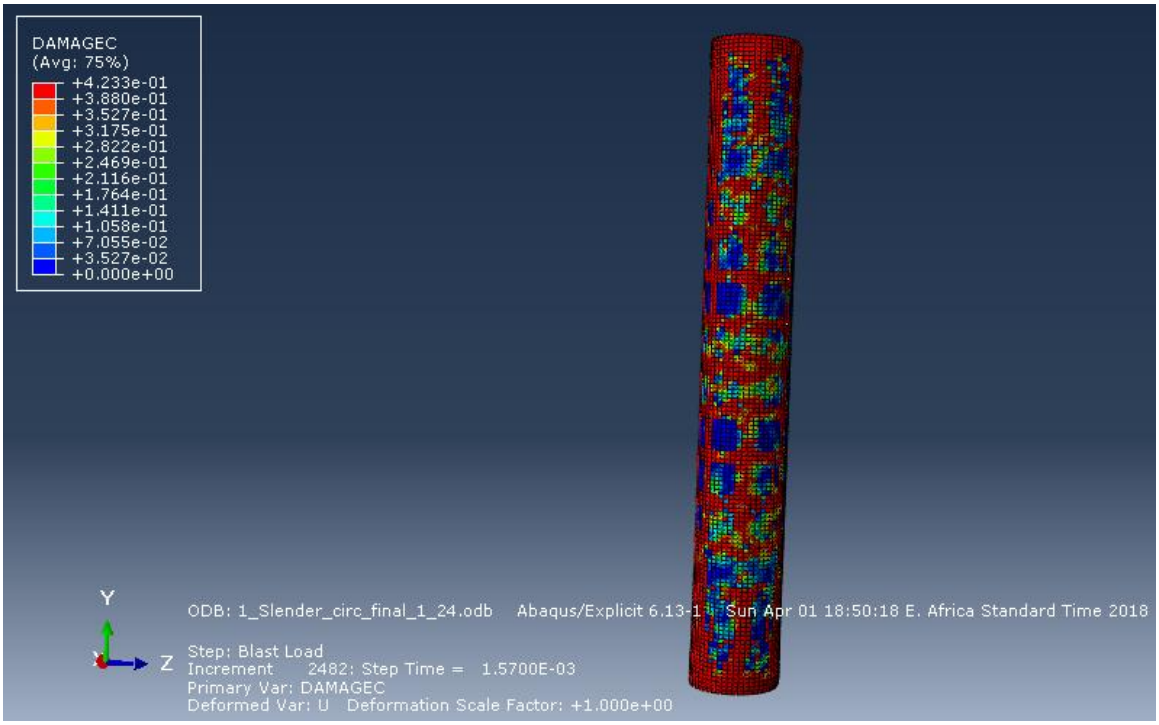

(d) Slender rectangular column DamageC

Figure 4.5 (a)-(d) Damagec for different column type at a scaled distance of $1.0\,ft/lb^{1/3}$

Figure 4.5 shows the DamageC of the four columns and the summary for the maximum deflection of each case is shown in Table 4.2. It shows short rectangular column produced smaller deflection whereas slender circular column produced larger lateral deflection compared to the other.

Table 4.2: Summary of Maximum deflection for different column types

Column Type	Max. Deflection (mm)
Short Rectangular	32.839
Short Circular	36.715
Slender Rectangular	39.209
Slender Circular	42.389

Short rectangular column, which is better than the others in resistance, is selected for further parametric study in the next parametric study.

4.3: Parametric Analysis

The parametric study investigates the combined effect of blast loading and axial loading on RC column detailed as shown in Figure 4.6. The numerical analysis was conducted with scaled distances of $0.5\ ft/lb^{1/3}$, $1\ ft/lb^{1/3}$ and $1.5\ ft/lb^{1/3}$. At each of these scaled distances charge masses of 100kg and 250kg were used at the corresponding standoff distances. The relationship between the scaled distance, Z, range, R, and the charge mass, W, is given by equation [4.1].

$$Z = \frac{R}{W^{1/3}} \qquad [4.1]$$

Using equation 4.1, the ranges for the Z values of $0.5\ ft/lb^{1/3}$, $1\ ft/lb^{1/3}$ and $1.5\ ft/lb^{1/3}$ are presented, in Table 4.3.

Table 4.3 Ranges and charge masses for the scaled distances

Scaled distance	Charge Mass (lb), (kg)	Standoff Distance (ft)	Transverse Spacing (mm)
$0.5\ ft/lb^{1/3}$	220.46 (100)	3.21	300
			200
			100
	551.16 (250)	4.36	300
			200
			100
$1.0\ ft/lb^{1/3}$	220.46 (100)	6.42	300
			200
			100
	551.16 (250	8.71	300
			200
			100
$1.5\ ft/lb^{1/3}$	220.46 (100)	9.63	300
			200

			100
	551.16 (250	13.07	300
			200
			100

For the purpose of parametric studies I have considered three columns with different transverse reinforcement spacing. For the first column type, designated as R1. The R1 RC columns had transverse reinforcement consisting of diameter 8mm ties spaced at 300 mm throughout the entire length of the column (Figure 4.6a). The second RC column type designation, R2, had transverse reinforcement spaced 200 mm throughout the entire length of the column (Figure 4.6b). The third RC column type designation, R3, had transverse reinforcement spaced 150 mm throughout the entire length of the column (Figure 4.6c).

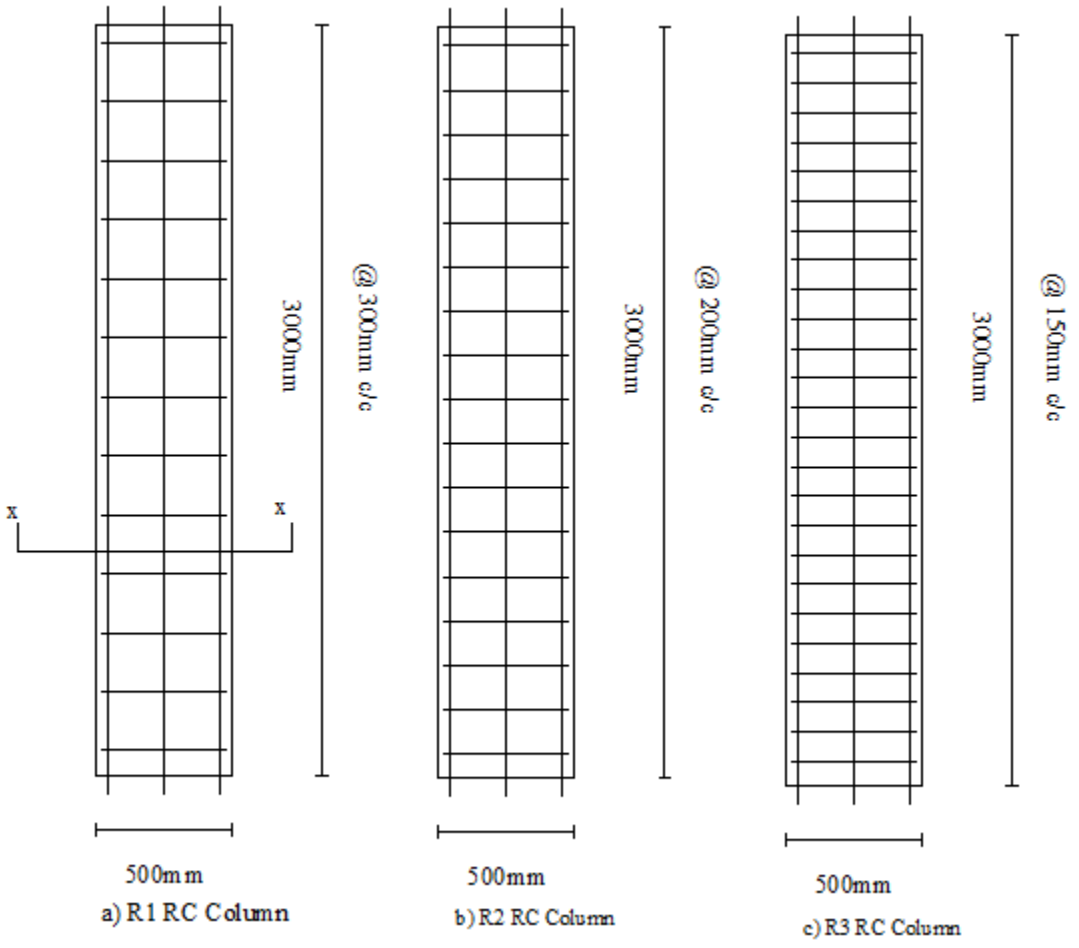

Figure 4.6: Three different RC column detailing used for numerical analysis

4.4. Effect of reinforcement detailing on column response

To study the effect of reinforcement detailing on the behavior of RC columns the short rectangular column with different transverse reinforcement spacing shown in Figure 4.6 is considered in all the three scaled distances of $0.5\ ft/lb^{1/3}$,$1.0\ ft/lb^{1/3}$ and $1.5\ ft/lb^{1/3}$.

4.4.1. Scaled distance of $0.5\ ft/lb^{1/3}$

Figure 4.7 and Figure 4.8 show the displacement-time histories of the three column types under blast loading from charge masses of 100 kg and 250 kg respectively at corresponding standoff distances for scaled distance of $0.5\ ft/lb^{1/3}$.

As we can see from Figure 4.7 the displacement produced by column designated as R1 and R2 are 84.963mm and 83.814mm which shows R2 column has a 1.3% reduced lateral deflection. Whereas R3 column produced 74.3mm which is 12.54% reduced lateral deflection compared to R1 column.

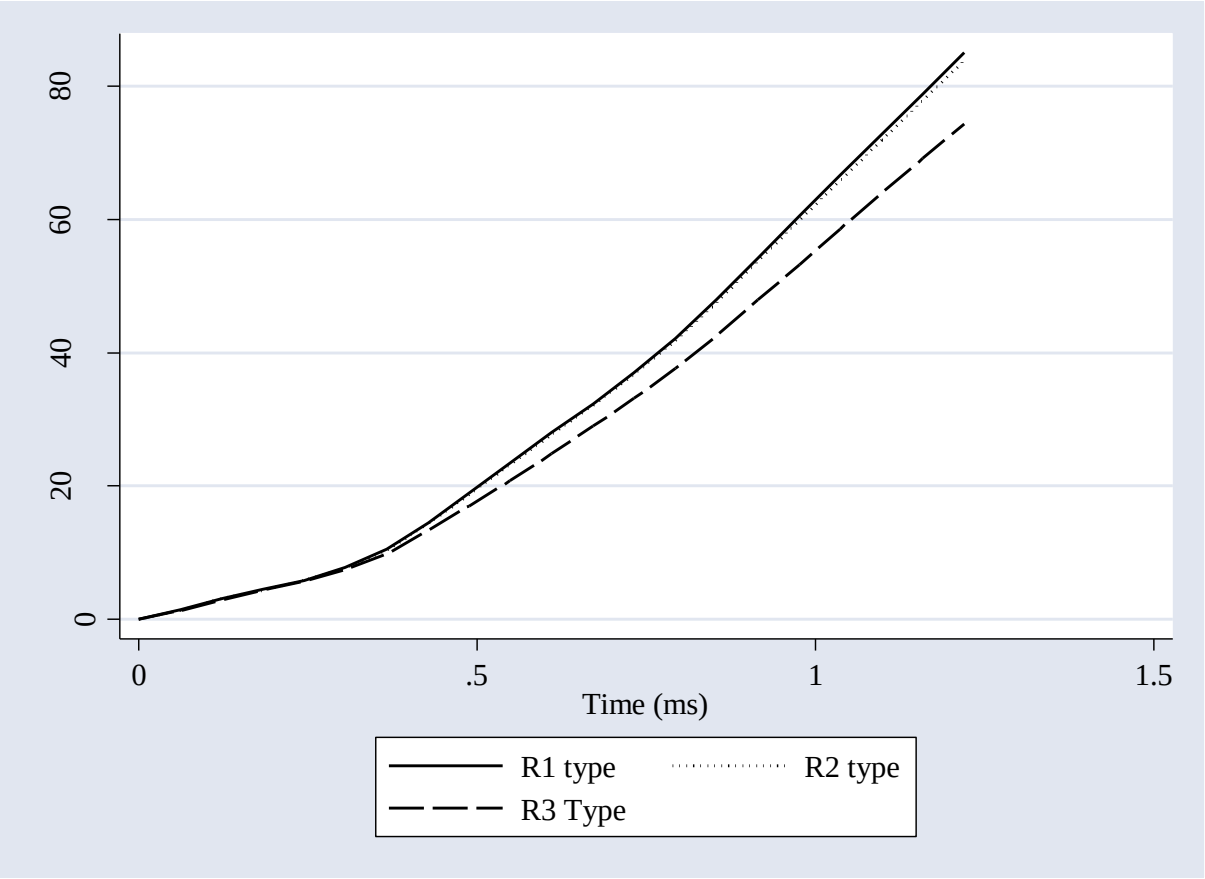

Figure 4.7 Displacement Time History at $0.5\ ft/lb^{1/3}$ using 100kg charge mass

For the 250-kg charge mass the lateral displacements, shown in Figure 4.8, were much higher for all three column types in comparison to the 100 kg charge mass, due to the higher impulse generated by the increased charge mass. The R1 and R2 columns produced 160.5mm and 157mm which approximately similar lateral deflection compared to R3 column which produced 139mm lateral displacement which implies R3 column type has 13.2% reduced deflection compared to R1 column type. Table 4.4 shows the summary of maximum lateral deflection of the three columns in both charge masses at a scaled distances of $0.5\ ft/lb^{1/3}$.

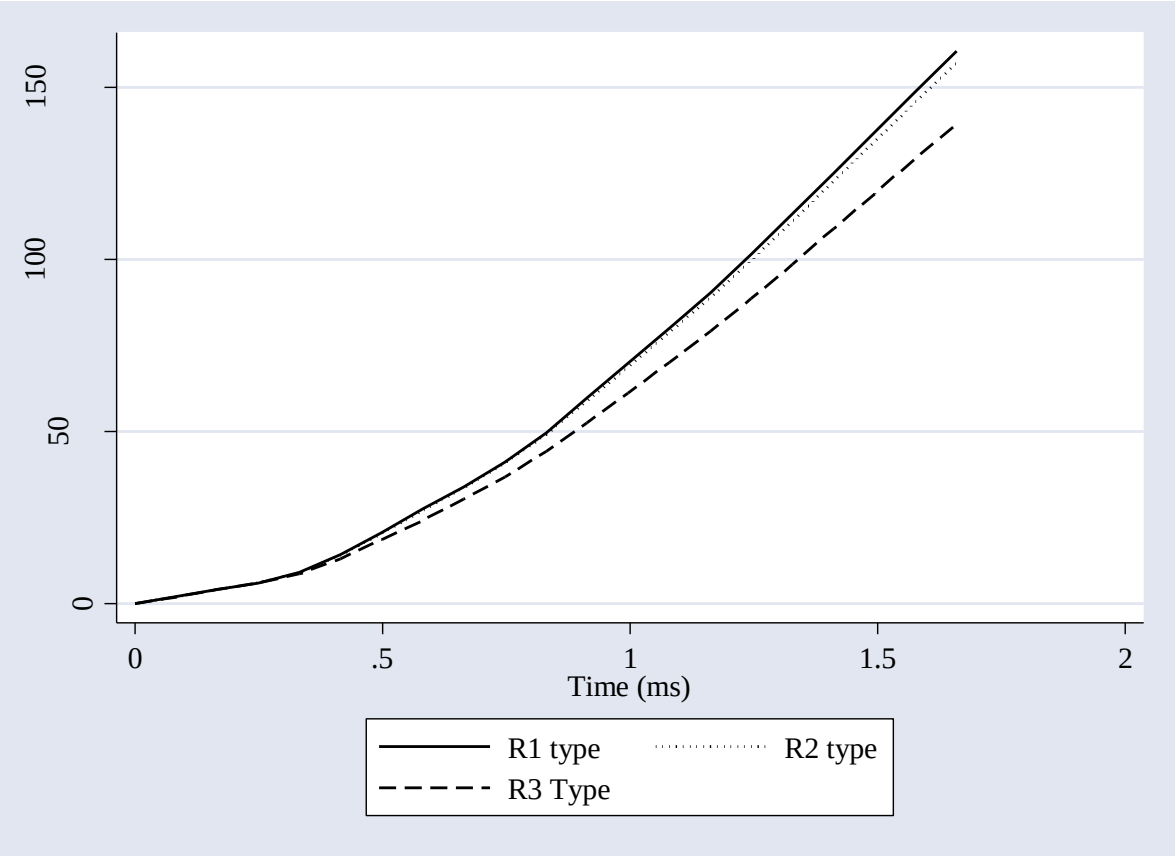

Figure 4.8 Displacement Time History at $0.5\ ft/lb^{1/3}$ using 250kg charge mass

Table 4.4 Summary of maximum lateral deflection at a scaled distance of $0.5\ ft/lb^{1/3}$

Charge Mass (kg)	R1 Type (mm)	R2 Type (mm)	R3 Type (mm)
100	84.963	83.814	74.306
250	160.544	157.245	139.291

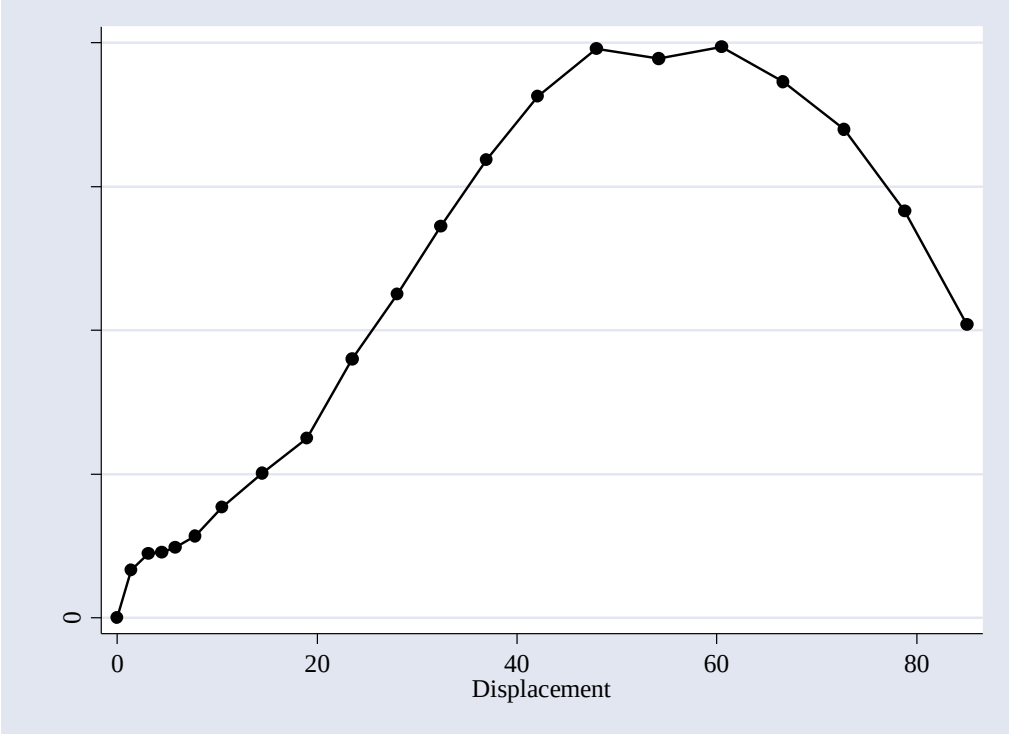

Figure 4.9 Reaction Vs Displacement at $0.5\ ft/lb^{1/3}$ using 100kg charge mass

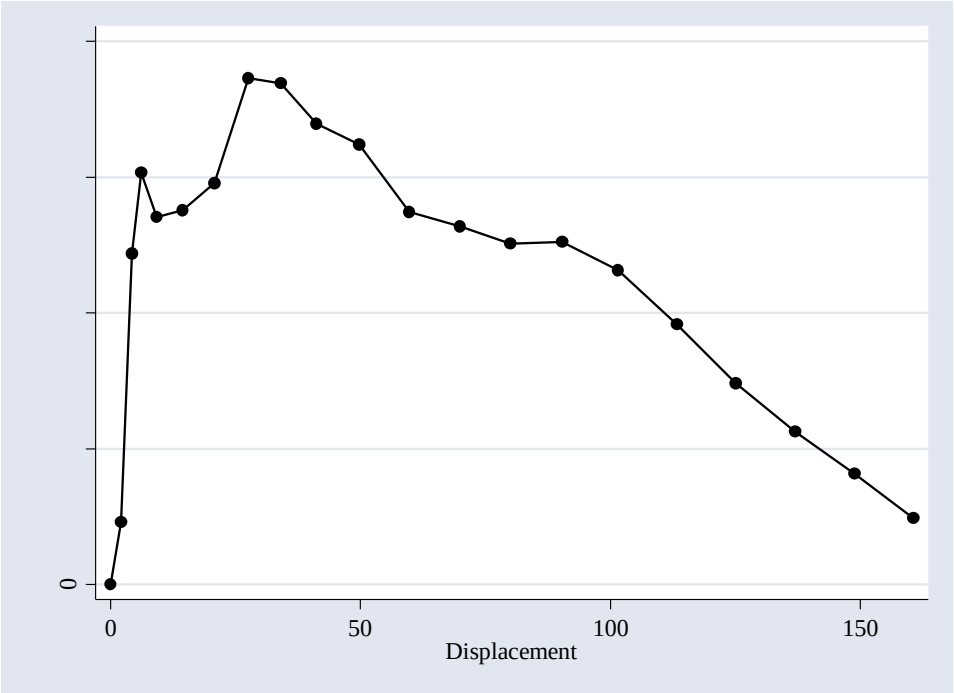

Figure 4.10 Reaction Vs Displacement at $0.5\ ft/lb^{1/3}$ using 250kg charge mass

Figure 4.9 and Figure 4.10 shows the Reaction at the support Vs Displacement at the middle at a scaled distance of $0.5\ ft/lb^{1/3}$ for both charge masses. In general I have experienced that increasing a charge mass will increase a lateral deflection of the column and also reducing the spacing between the stirrups will reduce the lateral displacement.

4.4.2. Scaled distance of $1.0\ ft/lb^{1/3}$

Figure 4.11 and Figure 4.12 show the displacement-time histories of the three column types under blast loading from charge masses of 100 kg and 250 kg respectively at corresponding standoff distances for scaled distance of $1.0\ ft/lb^{1/3}$.

In 100kg charge mass the displacement produced by column designated as R1 and R2 are approximately equal to 17mm. But column R3 produced 15.67mm which is 8.2% reduced lateral displacement compared to R1 column as seen from Figure 4.11.

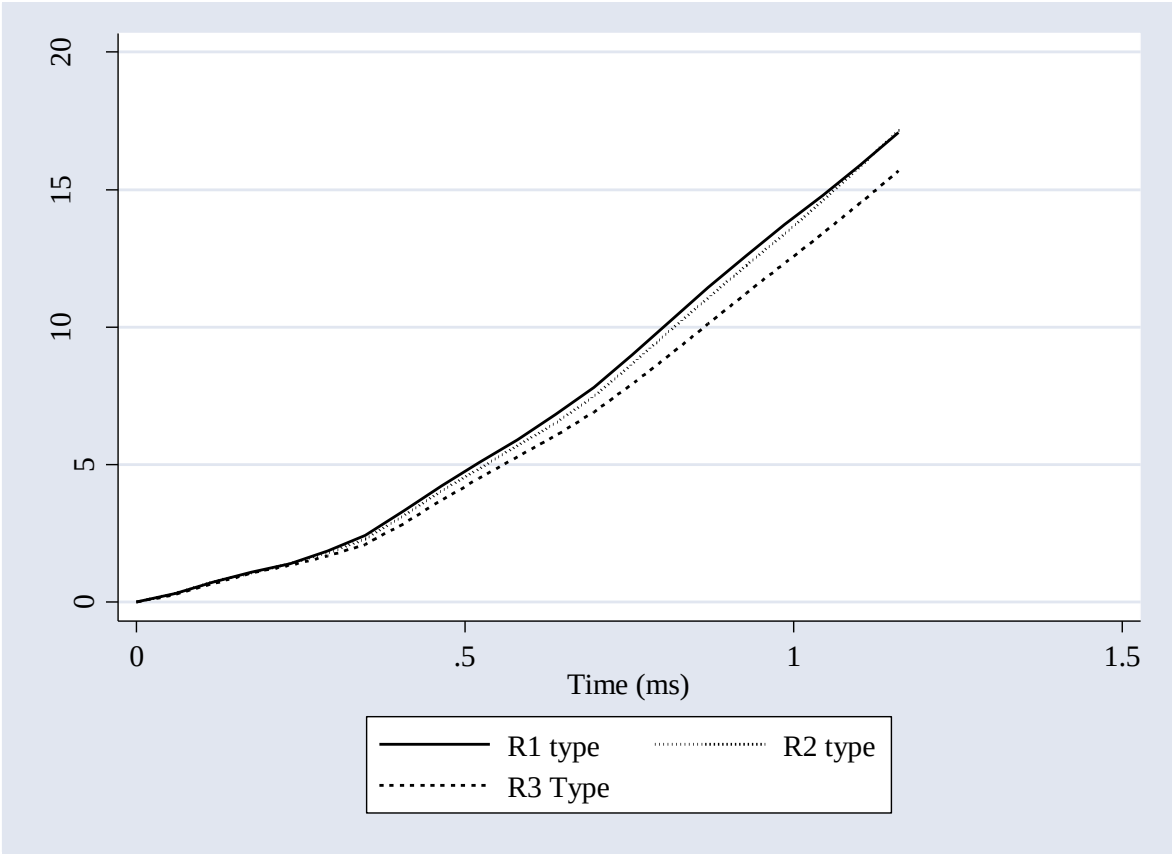

Figure 4.11 Displacement Time History at $1.0\ ft/lb^{1/3}$ using 100kg charge mass

In 250kg charge mass the displacement produced by R1 and R2 columns are approximately equal to 32.272mm. Column R3 produced 29.101mm lateral deflection which is 9.8% smaller deflection compared to R1 column Figure 4.12.

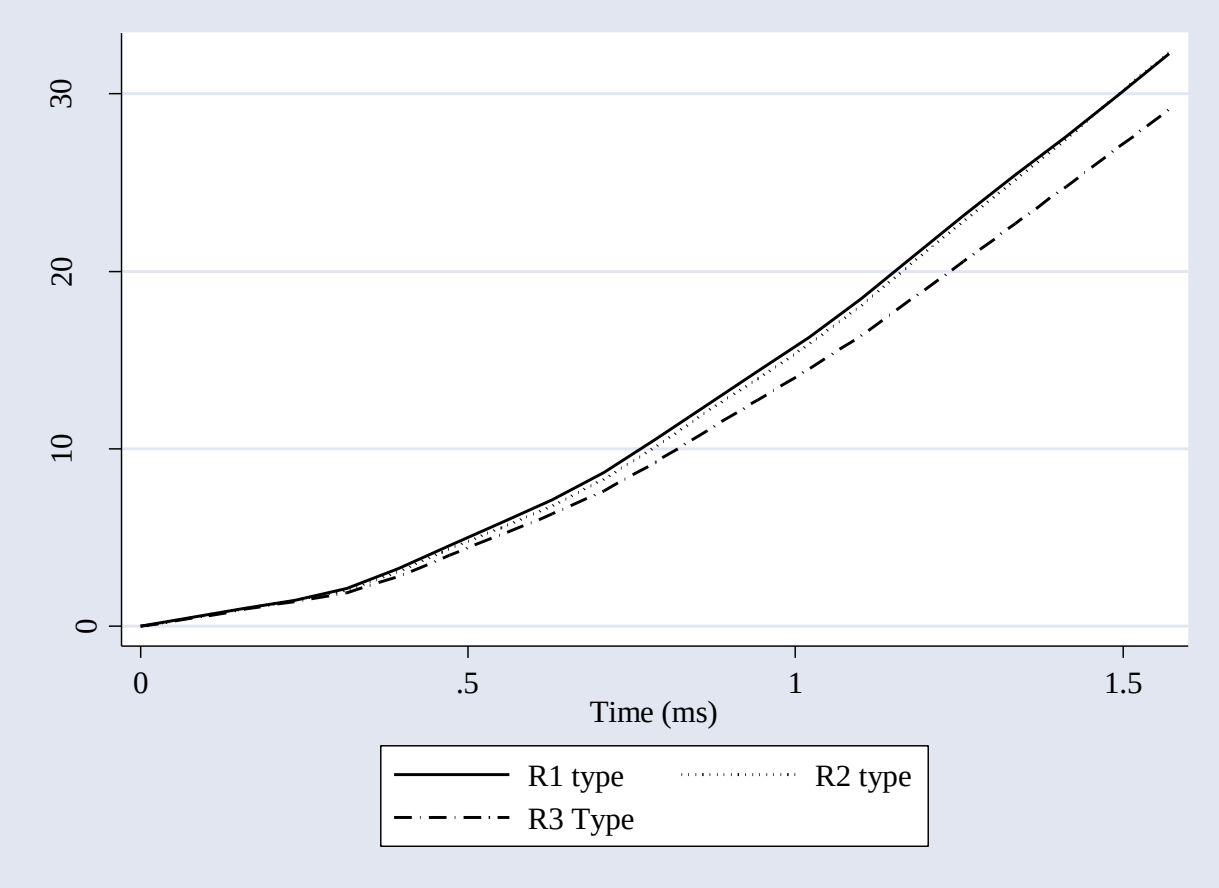

Figure 4.12 Displacement Time History at $1.0\ ft/lb^{1/3}$ using 250kg charge mass

Table 4.5 shows the maximum deflection of the three column at a scaled distance of $1.0\ ft/lb^{1/3}$ for both 100kg and 250kg charge masses.

Table 4.5 Summary of maximum lateral deflection at a scaled distance of $1.0\ ft/lb^{1/3}$

Charge Mass (kg)	R1 Type (mm)	R2 Type (mm)	R3 Type (mm)
100	17.068	17.152	15.672
250	32.272	32.322	29.101

Generally, we can conclude that increasing the scaled distance will decrease the lateral deflection of the columns significantly. In this scaled distance decreasing the stirrup spacing will decrease the lateral deflection with small value compared to $0.5\ ft/lb^{1/3}$ scaled distance case.

4.4.3. Scaled distance of $1.5\ ft/lb^{1/3}$

Figure 4.13 and Figure 4.14 show the displacement-time histories of the three column types under blast loading from charge masses of 100 kg and 250 kg respectively at corresponding standoff distances for scaled distance of $1.5\ ft/lb^{1/3}$. Table 4.6 shows the maximum displacement of the columns for both charge masses at a scaled distance of $1.5\ ft/lb^{1/3}$.

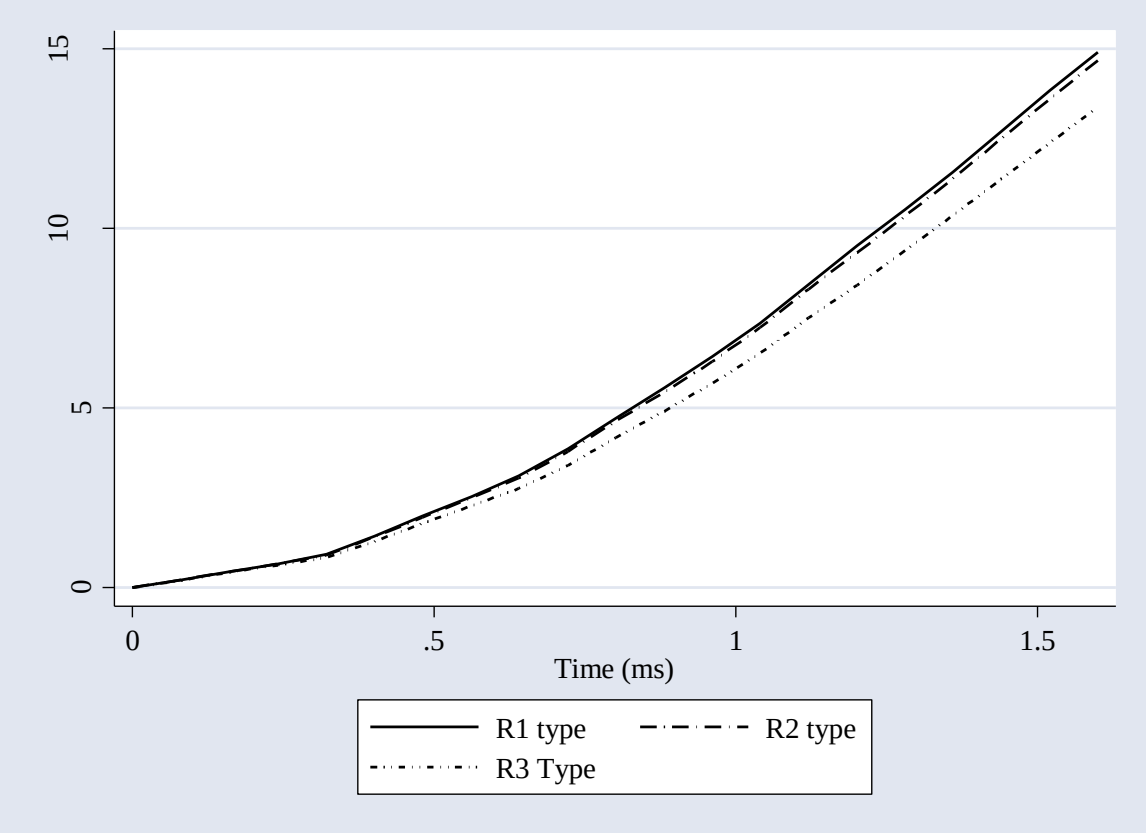

Figure 4.13 Displacement Time History at $1.5\ ft/lb^{1/3}$ using 100kg charge mass

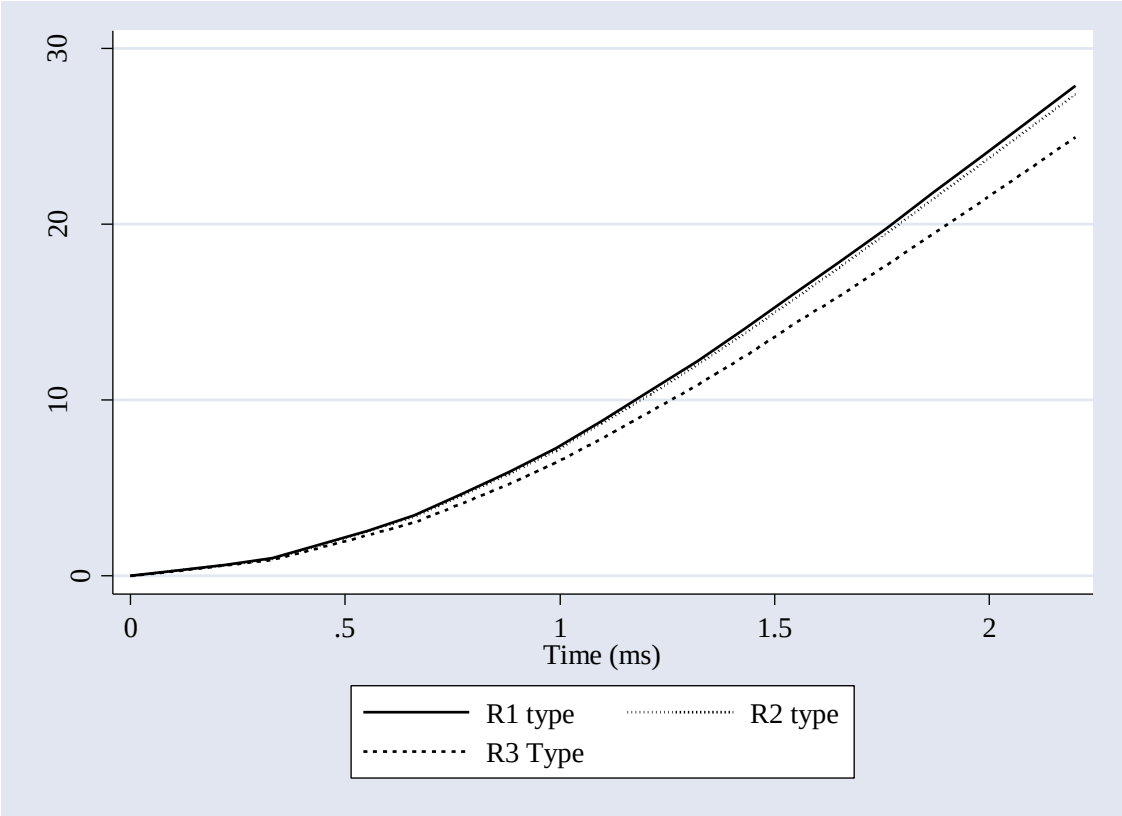

Figure 4.14 Displacement Time History at $1.5\ ft/lb^{1/3}$ using 250kg charge mass

In both charge masses the response of the columns is very similar with marginal differences in the recorded maximum displacement values as seen in Figure 4.13 and Figure 4.14. We can also see that decreasing the spacing of transverse reinforcement will have small effect at higher scaled distance than $1.5\ ft/lb^{1/3}$. Also we can conclude that the lateral deflection of the columns will decrease as the scaled distance increases.

Table 4.6 shows the summary of maximum deflection of the three column at a scaled distance of $1.0\ ft/lb^{1/3}$ for both 100kg and 250kg charge masses.

Table 4.6 Summary of maximum lateral deflection at a scaled distance of $1.5\ ft/lb^{1/3}$

Charge Mass (kg)	R1 Type (mm)	R2 Type (mm)	R3 Type (mm)
100	14.913	14.677	13.379
250	27.887	27.396	24.938

4.5. Effect of Axial Load Ratios on column response

The combined effect of blast and axial loading is studied at $1.0\ ft/lb^{1/3}$ scaled distance, and for 100kg and 250kg charge masses with ALRs of 0.0, 0.05, 0.15 and 0.25 were applied to the columns. The ALRs used were representative of gravity loading on lower storey RC columns for a building as well as for bridge piers. The axial load capacity for RC column by adding the contributions of concrete and steel reinforcement is computed based on EBCs 2 by using equation [4.2] and the computed factored axial load capacity, P_{ult} was 6737.53KN.

$$P_{ult} = f_{cd}(A_g - A_{st}) + f_{yd}A_{st} \qquad [4.2]$$

The axial load ratios (ALRs) used in this thesis were taken to be the ratio of the factored concentric axial load acting on the RC column, P, to the factored axial load capacity, P_{ult}, of the RC column given by equation [4.3]

$$ALR = \frac{P}{P_{ult}} \qquad [4.3]$$

Thus, for a given ALR, the load applied to the reinforced concrete column can then be computed using equation [4.4]

$$P = ALR. \times P_{ult} \qquad [4.4]$$

Table 4.7 shows the applied axial load based on different ALR.

Table 4.7 Applied axial loads for different axial load ratios

Axial Load Ratio (ALR)	Applied Axial Load (KN)
0.05	336.88
0.10	673.75
0.15	1010.63
0.25	1684.38

The R1 RC column type was subjected to 100-kg and 250-kg charge masses while the RC column was simultaneously subjected to different axial load ratios.

Figure 4.15 and Figure 4.16 show the displacement-time histories of the R1 column type under combined blast and axial loading from charge masses of 100 kg and 250 kg respectively at corresponding standoff distances for scaled distance of $1.0\ ft/lb^{1/3}$.

We can see from Figure 4.15 that using axial load will decrease the maximum displacement significantly, which is from 39.886 at ALRs of 0 to 23.683 at ALRs of 0.05. Similarly from Figure 4.16 the maximum displacement will be reduced from 70.375mm to 40.197mm.

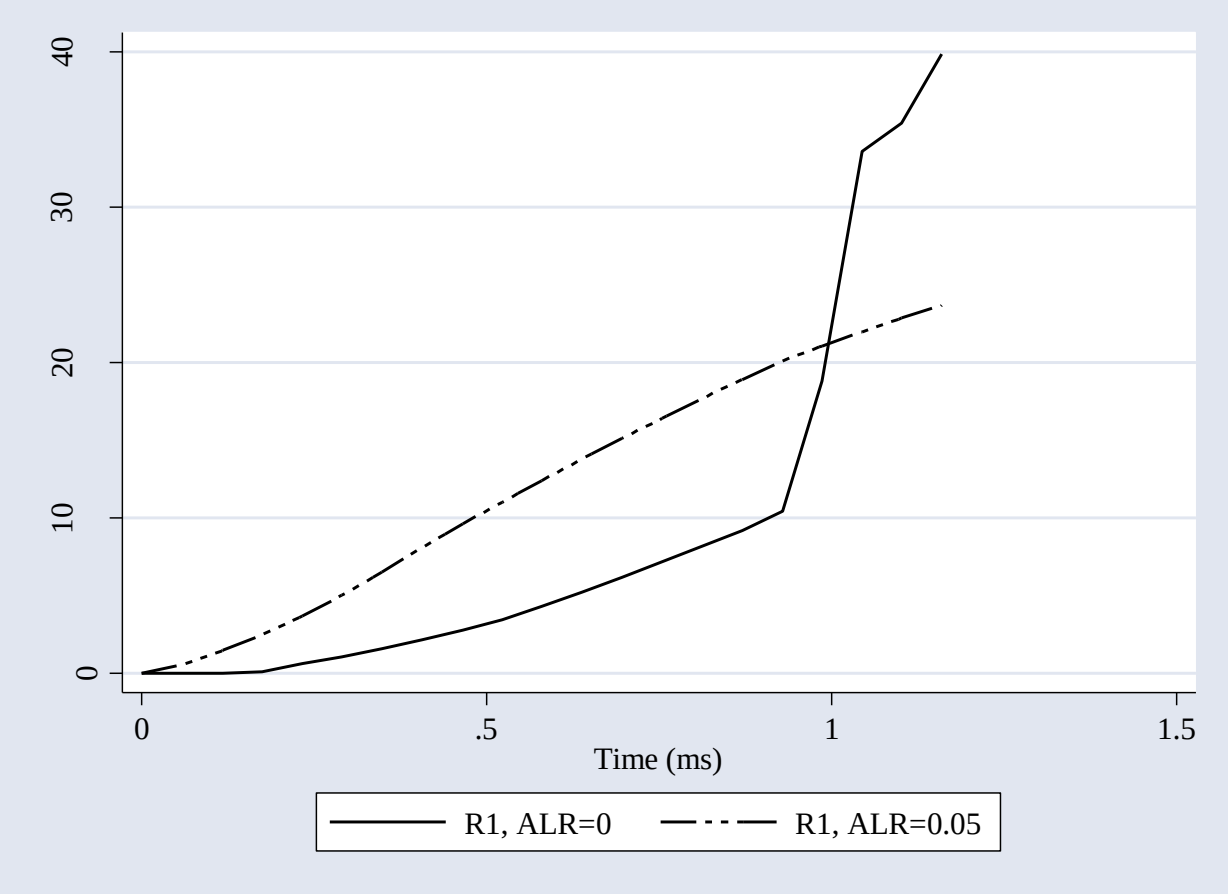

Figure 4.15 Displacement Vs Time History at $1.0\ ft/lb^{1/3}$ using 100kg charge mass

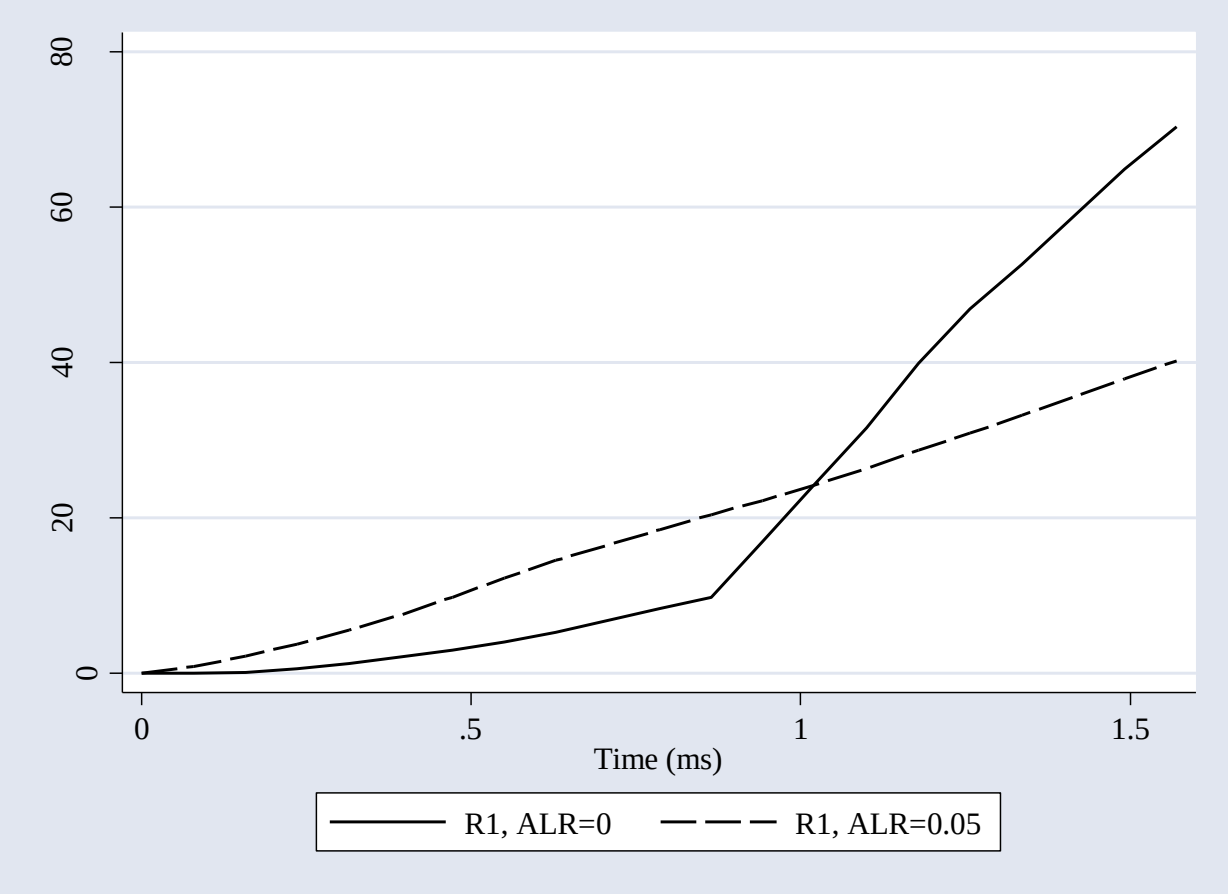

Figure 4.16 Displacement Vs Time History at 1.0 $ft/lb^{1/3}$ using 250kg charge mass

Table 4.8 shows the maximum deflection of the three column for combined blast and axial loadings at a scaled distance of 1.0 $ft/lb^{1/3}$ for both 100kg and 250kg charge masses.

Table 4.8 Summary of the maximum displacement for combined blast and axial loadings

Charge Mass	ALRs = 0	ALRs = 0.05	ALRs = 0.1	ALRs = 0.15	ALRs = 0.25
100kg	39.886	23.683	22.876	22.859	22.865
250kg	70.375	40.197	40.231	40.312	40.426

Generally, we can conclude that increasing the ALRs beyond 0.1 will not make much change in the deflection, it's similar compared to ALRs of 0.05.

Chapter Five: Conclusion and Recommendation

5.1. Conclusion

Based on the studies available in the literature, the ultimate objective is to know what the effect of conventional columns will be when subjected to sudden blast loading.

The following observations and conclusions are drawn from this study

- ✓ Rectangular column cross-section produced smaller lateral displacement compared to the circular column cross-section. Which implies rectangular column has greater stiffness than circular columns.
- ✓ Short column in both cross-section produced smaller lateral displacement compared to slender column. So short columns will have larger stiffness than slender column.
- ✓ Reduction of transverse reinforcement spacing in RC columns resulted in reduced lateral displacements at all scaled distances. But reducing the lateral reinforcement spacing will have small effect at large scaled distance.
- ✓ Increasing the scaled distance at the same charge mass will decrease the columns lateral deflection.
- ✓ The gravity loads from upper stories on the behavior of RC columns subjected to blast loading has reduced the lateral displacement in general.
- ✓ Generally, at the same scaled distance, increasing the magnitude of charge masses resulted in increased lateral displacement.

5.2. Recommendation

- ✓ There is the need to extend the parametric studies to include different column sizes as well as different longitudinal reinforcement schemes.
- ✓ There is also the need to extend the parametric study to include different column shape other than the rectangular and circular cross-section.
- ✓ The longitudinal bars were modelled as continuous throughout the entire length of the columns. The effect of longitudinal reinforcement lapping that usually occurs within RC column support regions needs to also be looked at.

Refference

1. Ngo, T., Mendis, P., Gupta, A., Ramasy, J. Blast Loading and Blast Effects on Structure. Electron J Struct Eng. 2007;(Loading on Structures):P.76-91.

2. Esper, P. Non-linear transient and Quasi-static Analyses of the Dynamic Response of Buildings to Blast Loading, ANSYS 7th International Conference and Exhibition on Finite Element Modelling and Analysis. Pittsburgh, USA; 1996.

3. Jayasooriya, R., Thambiratnam, D., Perera, N, Kosse, V. Response and Damage evaluation of reinforced concrete frames subjected to blast loading. In: 34th Conference on Our World in Concrete and Structures. Hotel Park Royal, Singapore; 2009. 16–18 p.

4. Marchand, K.A., Alfawakhiri, F. Blast and Progressive Collapse. American Institute of Steel Construction; 2005.

5. TM 5-1300(UFC 3-340-02) U.S. Army Corps of Engineers. Structures to Resist the Effects of Accidental Explosions. U.S. Army Corps of Engineers, Washington, D.C; 1990.

6. Yandzio E., Gough M. Protection of Buildings against Explosions, Steel Construction Institute. 1999.

7. Kleine, H., Dewey, J.M., Ohashi, K., Mizukaki, T., Takayama, K. Studies of the TNT equivalence of silver azide charges. Shock Waves. 2003;13(2):123–38.

8. Cooper, P.W. Comments on TNT equivalence. Alburquerque, United State; 1994.

9. Held, M. TNT-Equivalent. Propellants, Explosives, Pyrotechnics. 1983;

10. Sochet, I. Blast effects of external explosions. Yokohama: Japan; 2010.

11. PEC, and BakerRisk. U.S. Army Corps of Engineers Protective Design Center Technical Report. 2008;

12. PAZ, M. Structural Dynamics Theory and Computation. Second Edition. Van Nostrand Reinhold Company; 1985.

13. Dusenberry, D.O. Handbook for Blast-Resistant Design of Buildings. Hoboken, New Jersey: JOHN WILEY & SONS, INC.; 2010.

14. Grote D., Park S. W., Zhou M. Dynamic Behaviour of Concrete at High Strain Rates and Pressures-I, Experimental Characterization. Int J Impact Eng. 2001;25(9):869–86.

15. Wight, J.K, Macgregor, J.G. Reinforced Concrete Mechanics and Design. Sixth Edition. New Jersey: Pearson Education, Inc.; 2008.

16. Malvar L., Crawford J. E. Dynamic Increase Factors for Concrete. Naval Facilities Engineering Service Center Port Hueneme, CA; 1998.

17. Farouk, S. Experimental program conducted to test near-field blast loading on reinforced concrete columns. Ottawa: Civil Engineering Department, Carleton University; 2013.

Appendix A

Figure A1: Positive Phase Shock Wave Parameter for a Spherical TNT Explosion in Free Air

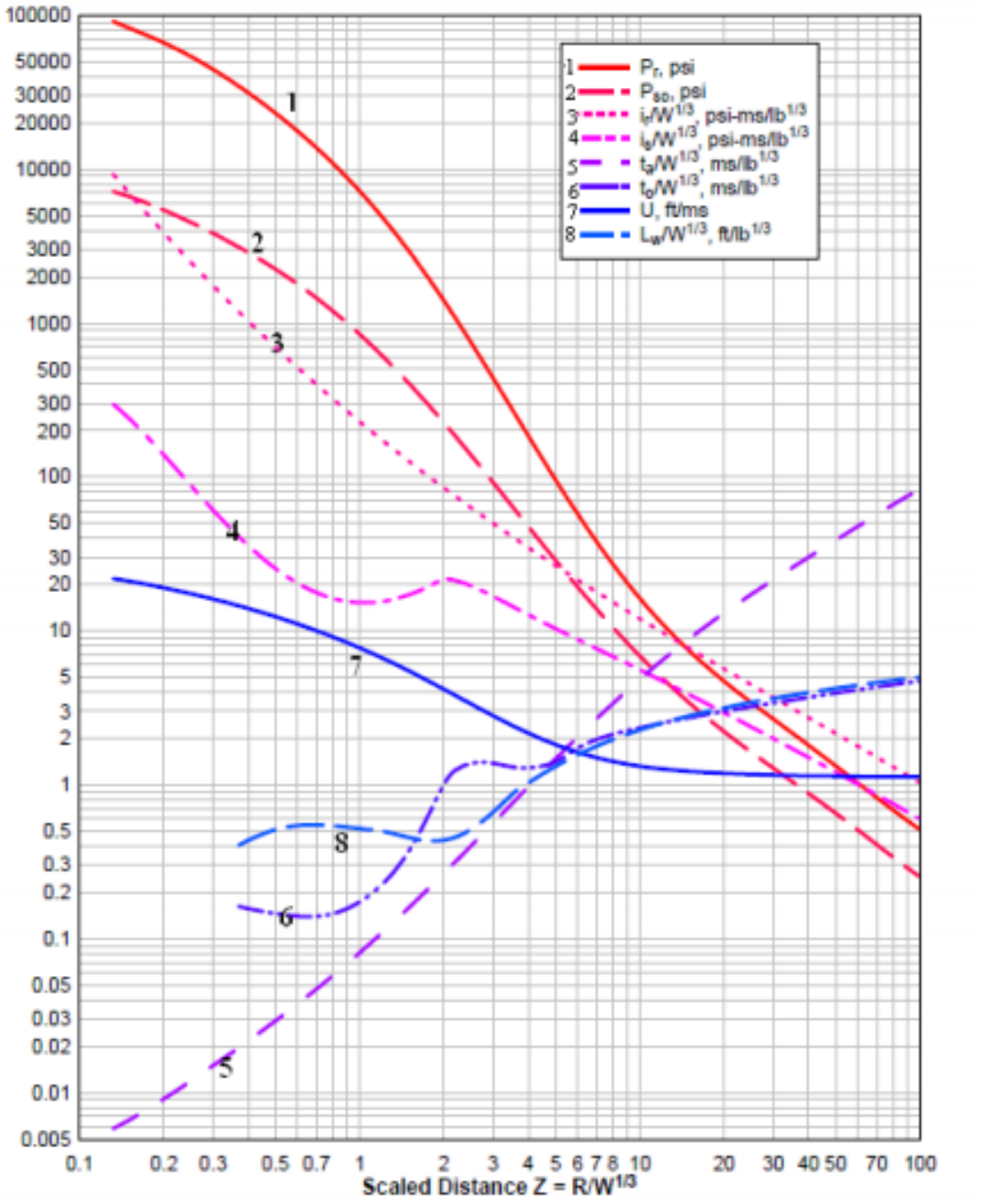

(a)

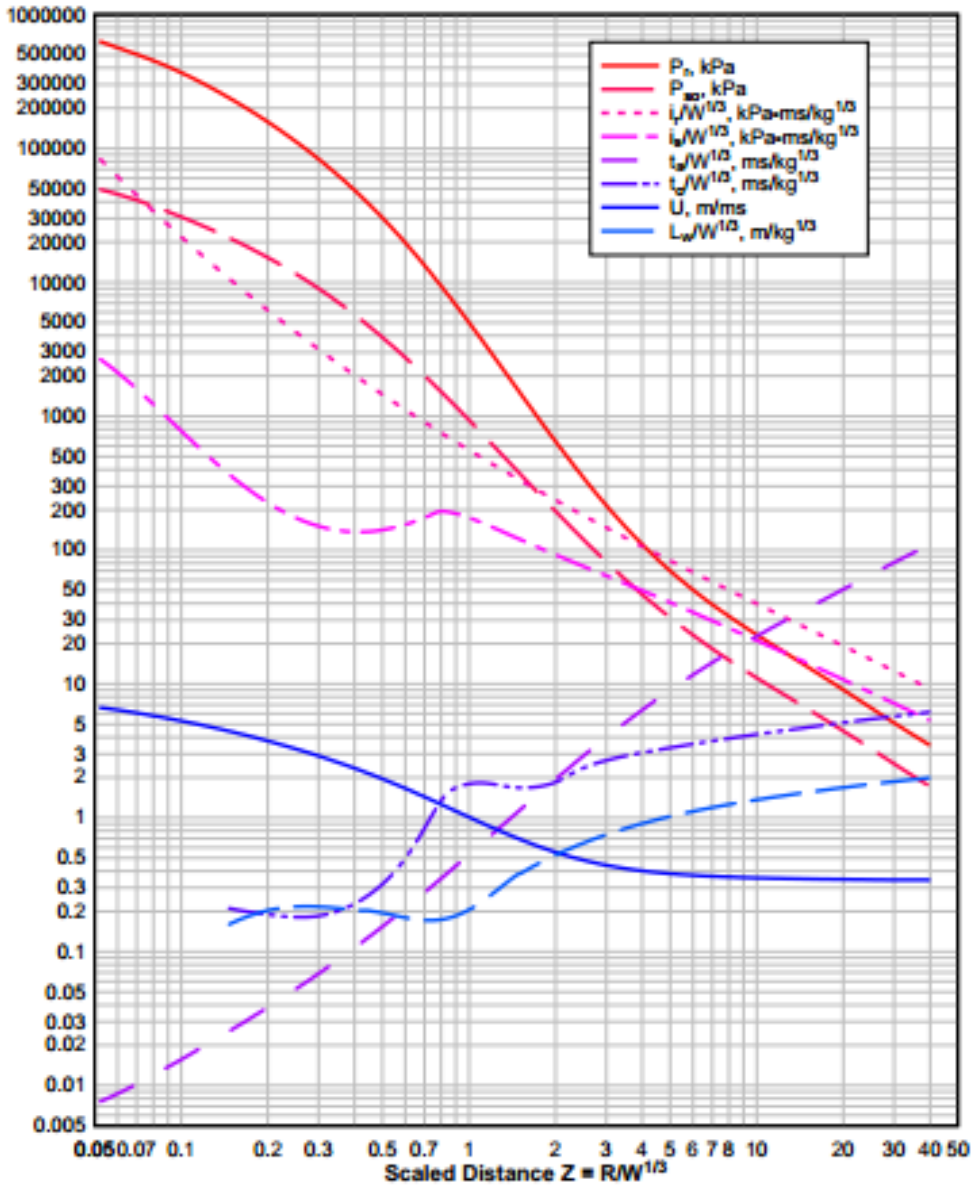

(b)

Procedure for determination of free-field blast wave parameters for a surface burst.

Step 1. Select point of interest on the ground relative to the charge. Determine the charge weight, and ground distance R_G.

Step 2. Apply a 20% safety factor to the charge weight.

Step 3. Calculate scaled ground distance Z_G.

$$Z_G = \frac{R_G}{W^{1/3}}$$

Step 4. Determine free-field blast wave parameters from figure_____ for corresponding scaled ground distance Z_G .

Read:

Reflected Pressure (P_r), Peak positive incident pressure (P_{so}), Shock front velocity (U_0), Scaled unit positive incident impulse ($i_s / W^{1/3}$), Scaled positive phase duration ($t_0 / W^{1/3}$) and Scaled arrival time ($t_A / W^{1/3}$). Then multiply scaled values by $W^{1/3}$ to obtain absolute value.

Appendix B

Table B1: Load mass factors for different support and Loading types

	Load Type	
Support Type	Uniformly Distributed Load	Point Load
Pinned-Pinned	0.72	0.41
Pinned-Fixed	0.72	0.395
Fixed-Fixed	0.7175	0.35
Fixed-Free	0.285	0.655

Table B2: Equivalent Stiffness values for different support and Loading types

	Load Type	
Support Type	Uniformly Distributed Load	Point Load
Pinned-Pinned	$\frac{384EI}{5L^4}$	$\frac{48EI}{L^3}$
Pinned-Fixed	$\frac{160EI}{L^4}$	$\frac{106EI}{L^3}$
Fixed-Fixed	$\frac{307EI}{L^4}$	$\frac{192EI}{L^3}$
Fixed-Free	$\frac{8EI}{L^4}$	$\frac{3EI}{L^3}$

The values of E and I are given by

$$E = 4500\sqrt{F_{dy}}$$

$$I = 0.5\left(I_{gt} + I_{cr}\right)$$

Where I_{gt} = the gross transformed moment of inertia.

I_{cr} = the cracked moment of inertia.

F_{dy} = dynamic flexural yield strength

Table B3: Ultimate resistance for different support and Loading types

	Load Type	
Support Type	Uniformly Distributed Load	Point Load
Pinned-Pinned	$\frac{8M_P}{L^2}$	$\frac{4M_P}{L}$
Pinned-Fixed	$\frac{4(M_n + 2M_P)}{L^2}$	$\frac{2(M_n + 2M_P)}{L}$
Fixed-Fixed	$\frac{8(M_n + 2M_P)}{L^2}$	$\frac{4(M_n + M_P)}{L}$
Fixed-Free	$\frac{2M_n}{L^2}$	$\frac{M_n}{L}$

$$M_n = F_{yd} A_{spos} \left(d - \frac{a}{2} \right)$$

$$M_P = F_{yd} A_{sneg} \left(d - \frac{a}{2} \right)$$

Where F_{yd} = dynamic flexural yield strength

A_{spos} = Area of steel in the compression region when column is under bending.

A_{sneg} = Area of steel in the tension region when column is under bending.

Appendix C

Data's related to part model is removed because they occupy large space.

*Heading

** Job name: Expermental_validation_1_20mm Model name: Model-1

** Generated by: Abaqus/CAE 6.13-1

*Preprint, echo=NO, model=NO, history=NO, contact=NO

**

** ASSEMBLY

**

*Assembly, name=Assembly

**

*Instance, name=Concrete-1, part=Concrete

100., 3000., 100.

100., 3000., 100., 101., 3000., 100., 90.

*End Instance

**

*Instance, name=Rebar-1, part=Rebar

290., 3050., 40.

290., 3050., 40., 290., 3050., 41., 90.

*End Instance

**

*Instance, name=Stirrup-1, part=Stirrup

140., 1500., 140.

140., 1500., 140., 141., 1500., 140., 90.

*End Instance

**

*Instance, name=Rebar-1-lin-1-2, part=Rebar

290., 3050., 260.

290., 3050., 260., 290., 3050., 261., 90.

*End Instance

**

*Instance, name=Rebar-1-lin-2-1, part=Rebar

510., 3050., 40.

510., 3050., 40., 510., 3050., 41., 90.

*End Instance

**

*Instance, name=Rebar-1-lin-2-2, part=Rebar

510., 3050., 260.

510., 3050., 260., 510., 3050., 261., 90.

*End Instance

**

*Instance, name=Stirrup-1-lin-1-2, part=Stirrup

140., 1575., 140.

140., 1575., 140., 141., 1575., 140., 90.

*End Instance

**

*Instance, name=Stirrup-1-lin-1-3, part=Stirrup

140., 1650., 140.

140., 1650., 140., 141., 1650., 140., 90.

*End Instance

**

*Instance, name=Stirrup-1-lin-1-4, part=Stirrup

140., 1725., 140.

140., 1725., 140., 141., 1725., 140., 90.

*End Instance

**

*Instance, name=Stirrup-1-lin-1-5, part=Stirrup

140., 1800., 140.

140., 1800., 140., 141., 1800., 140., 90.

*End Instance

**

*Instance, name=Stirrup-1-lin-2-1, part=Stirrup

140., 1425., 140.

140., 1425., 140., 141., 1425., 140., 90.

*End Instance

**

*Instance, name=Stirrup-1-lin-2-2, part=Stirrup

140., 1500., 140.

140., 1500., 140., 141., 1500., 140., 90.

*End Instance

**

*Instance, name=Stirrup-1-lin-2-3, part=Stirrup

140., 1575., 140.

140., 1575., 140., 141., 1575., 140., 90.

*End Instance

**

*Instance, name=Stirrup-1-lin-2-4, part=Stirrup

140., 1650., 140.

140., 1650., 140., 141., 1650., 140., 90.

*End Instance

**

*Instance, name=Stirrup-1-lin-2-5, part=Stirrup

140., 1725., 140.

140., 1725., 140., 141., 1725., 140., 90.

*End Instance

**

*Instance, name=Stirrup-1-lin-3-1, part=Stirrup

140., 1350., 140.

140., 1350., 140., 141., 1350., 140., 90.

*End Instance

**

*Instance, name=Stirrup-1-lin-3-2, part=Stirrup

140., 1425., 140.

140., 1425., 140., 141., 1425., 140., 90.

*End Instance

**

*Instance, name=Stirrup-1-lin-3-3, part=Stirrup

140., 1500., 140.

140., 1500., 140., 141., 1500., 140., 90.

*End Instance

**

*Instance, name=Stirrup-1-lin-3-4, part=Stirrup

140., 1575., 140.

140., 1575., 140., 141., 1575., 140., 90.

*End Instance

**

*Instance, name=Stirrup-1-lin-3-5, part=Stirrup

140., 1650., 140.

140., 1650., 140., 141., 1650., 140., 90.

*End Instance

**

*Instance, name=Stirrup-1-lin-4-1, part=Stirrup

140., 1275., 140.

140., 1275., 140., 141., 1275., 140., 90.

*End Instance

**

*Instance, name=Stirrup-1-lin-4-2, part=Stirrup

140., 1350., 140.

140., 1350., 140., 141., 1350., 140., 90.

*End Instance

**

*Instance, name=Stirrup-1-lin-4-3, part=Stirrup

140., 1425., 140.

140., 1425., 140., 141., 1425., 140., 90.

*End Instance

**

*Instance, name=Stirrup-1-lin-4-4, part=Stirrup

140., 1500., 140.

140., 1500., 140., 141., 1500., 140., 90.

*End Instance

**

*Instance, name=Stirrup-1-lin-4-5, part=Stirrup

140., 1575., 140.

140., 1575., 140., 141., 1575., 140., 90.

*End Instance

**

*Instance, name=Stirrup-1-lin-5-1, part=Stirrup

140., 1200., 140.

140., 1200., 140., 141., 1200., 140., 90.

*End Instance

**

*Instance, name=Stirrup-1-lin-5-2, part=Stirrup

140., 1275., 140.

140., 1275., 140., 141., 1275., 140., 90.

*End Instance

**

*Instance, name=Stirrup-1-lin-5-3, part=Stirrup

140., 1350., 140.

140., 1350., 140., 141., 1350., 140., 90.

*End Instance

**

*Instance, name=Stirrup-1-lin-5-4, part=Stirrup

140., 1425., 140.

140., 1425., 140., 141., 1425., 140., 90.

*End Instance

**

*Instance, name=Stirrup-1-lin-5-5, part=Stirrup

140., 1500., 140.

140., 1500., 140., 141., 1500., 140., 90.

*End Instance

**

*Instance, name=Stirrup-1-lin-1-5-lin-1-2, part=Stirrup

140., 1950., 140.

140., 1950., 140., 141., 1950., 140., 90.

*End Instance

**

*Instance, name=Stirrup-1-lin-1-5-lin-1-3, part=Stirrup

140., 2100., 140.

140., 2100., 140., 141., 2100., 140., 90.

*End Instance

**

*Instance, name=Stirrup-1-lin-1-5-lin-1-4, part=Stirrup

140., 2250., 140.

140., 2250., 140., 141., 2250., 140., 90.

*End Instance

**

*Instance, name=Stirrup-1-lin-1-5-lin-1-5, part=Stirrup

140., 2400., 140.

140., 2400., 140., 141., 2400., 140., 90.

*End Instance

**

*Instance, name=Stirrup-1-lin-1-5-lin-1-5-lin-1-2, part=Stirrup

140., 2475., 140.

140., 2475., 140., 141., 2475., 140., 90.

*End Instance

**

*Instance, name=Stirrup-1-lin-1-5-lin-1-5-lin-1-3, part=Stirrup

140., 2550., 140.

140., 2550., 140., 141., 2550., 140., 90.

*End Instance

**

*Instance, name=Stirrup-1-lin-1-5-lin-1-5-lin-1-4, part=Stirrup

140., 2625., 140.

140., 2625., 140., 141., 2625., 140., 90.

*End Instance

**

*Instance, name=Stirrup-1-lin-1-5-lin-1-5-lin-1-5, part=Stirrup

140., 2700., 140.

140., 2700., 140., 141., 2700., 140., 90.

*End Instance

**

*Instance, name=Stirrup-1-lin-1-5-lin-1-5-lin-1-6, part=Stirrup

140., 2775., 140.

140., 2775., 140., 141., 2775., 140., 90.

*End Instance

**

*Instance, name=Stirrup-1-lin-1-5-lin-1-5-lin-1-7, part=Stirrup

140., 2850., 140.

140., 2850., 140., 141., 2850., 140., 90.

*End Instance

**

*Instance, name=Stirrup-1-lin-1-5-lin-1-5-lin-1-8, part=Stirrup

140., 2925., 140.

140., 2925., 140., 141., 2925., 140., 90.

*End Instance

**

*Instance, name=Stirrup-1-lin-1-5-lin-1-5-lin-1-9, part=Stirrup

140., 3000., 140.

140., 3000., 140., 141., 3000., 140., 90.

*End Instance

**

*Instance, name=Stirrup-1-lin-5-1-lin-1-2, part=Stirrup

140., 1050., 140.

140., 1050., 140., 141., 1050., 140., 90.

*End Instance

**

*Instance, name=Stirrup-1-lin-5-1-lin-1-3, part=Stirrup

140., 900., 140.

140., 900., 140., 141., 900., 140., 90.

*End Instance

**

*Instance, name=Stirrup-1-lin-5-1-lin-1-4, part=Stirrup

140., 750., 140.

140., 750., 140., 141., 750., 140., 90.

*End Instance

**

*Instance, name=Stirrup-1-lin-5-1-lin-1-5, part=Stirrup

140., 600., 140.

140., 600., 140., 141., 600., 140., 90.

*End Instance

**

*Instance, name=Stirrup-1-lin-5-1-lin-1-5-lin-1-2, part=Stirrup

140., 525., 140.

140., 525., 140., 141., 525., 140., 90.

*End Instance

**

*Instance, name=Stirrup-1-lin-5-1-lin-1-5-lin-1-3, part=Stirrup

140., 450., 140.

140., 450., 140., 141., 450., 140., 90.

*End Instance

**

*Instance, name=Stirrup-1-lin-5-1-lin-1-5-lin-1-4, part=Stirrup

140., 375., 140.

140., 375., 140., 141., 375., 140., 90.

*End Instance

**

*Instance, name=Stirrup-1-lin-5-1-lin-1-5-lin-1-5, part=Stirrup

140., 300., 140.

140., 300., 140., 141., 300., 140., 90.

*End Instance

**

*Instance, name=Stirrup-1-lin-5-1-lin-1-5-lin-1-6, part=Stirrup

140., 225., 140.

140., 225., 140., 141., 225., 140., 90.

*End Instance

**

*Instance, name=Stirrup-1-lin-5-1-lin-1-5-lin-1-7, part=Stirrup

140., 150., 140.

140., 150., 140., 141., 150., 140., 90.

*End Instance

**

*Instance, name=Stirrup-1-lin-5-1-lin-1-5-lin-1-8, part=Stirrup

140., 75., 140.

140., 75., 140., 141., 75., 140., 90.

*End Instance

**

*Instance, name=Stirrup-1-lin-5-1-lin-1-5-lin-1-9, part=Stirrup

140., 0., 140.

140., 0., 140., 141., 0., 140., 90.

*End Instance

**

*Nset, nset=_PickedSet110, internal, instance=Rebar-1, generate

1, 151, 1

*Nset, nset=_PickedSet110, internal, instance=Stirrup-1, generate

1, 44, 1

*Nset, nset=_PickedSet110, internal, instance=Rebar-1-lin-1-2, generate

1, 151, 1

*Nset, nset=_PickedSet110, internal, instance=Stirrup-1-lin-1-3, generate

1, 44, 1

*Nset, nset=_PickedSet110, internal, instance=Stirrup-1-lin-3-1, generate

1, 44, 1

*Nset, nset=_PickedSet110, internal, instance=Stirrup-1-lin-1-5-lin-1-3, generate

1, 44, 1

*Nset, nset=_PickedSet110, internal, instance=Stirrup-1-lin-5-1-lin-1-5-lin-1-3, generate

1, 44, 1

*Nset, nset=_PickedSet110, internal, instance=Stirrup-1-lin-4-4, generate

1, 44, 1

*Nset, nset=_PickedSet110, internal, instance=Stirrup-1-lin-1-5-lin-1-5-lin-1-7, generate

1, 44, 1

*Nset, nset=_PickedSet110, internal, instance=Stirrup-1-lin-2-2, generate

1, 44, 1

*Nset, nset=_PickedSet110, internal, instance=Stirrup-1-lin-3-5, generate

1, 44, 1

*Nset, nset=_PickedSet110, internal, instance=Stirrup-1-lin-1-5-lin-1-5-lin-1-3, generate

1, 44, 1

*Nset, nset=_PickedSet110, internal, instance=Stirrup-1-lin-5-1-lin-1-5-lin-1-7, generate

1, 44, 1

*Nset, nset=_PickedSet110, internal, instance=Stirrup-1-lin-5-3, generate

1, 44, 1

*Nset, nset=_PickedSet110, internal, instance=Stirrup-1-lin-5-1-lin-1-3, generate

1, 44, 1

*Nset, nset=_PickedSet110, internal, instance=Rebar-1-lin-2-2, generate

1, 151, 1

*Nset, nset=_PickedSet110, internal, instance=Stirrup-1-lin-1-5, generate

1, 44, 1

*Nset, nset=_PickedSet110, internal, instance=Stirrup-1-lin-3-3, generate

1, 44, 1

*Nset, nset=_PickedSet110, internal, instance=Stirrup-1-lin-1-5-lin-1-5, generate

1, 44, 1

*Nset, nset=_PickedSet110, internal, instance=Stirrup-1-lin-5-1-lin-1-5-lin-1-5, generate

1, 44, 1

*Nset, nset=_PickedSet110, internal, instance=Stirrup-1-lin-5-1, generate

1, 44, 1

*Nset, nset=_PickedSet110, internal, instance=Stirrup-1-lin-1-5-lin-1-5-lin-1-9, generate

1, 44, 1

*Nset, nset=_PickedSet110, internal, instance=Stirrup-1-lin-2-4, generate

1, 44, 1

*Nset, nset=_PickedSet110, internal, instance=Stirrup-1-lin-4-2, generate

1, 44, 1

*Nset, nset=_PickedSet110, internal, instance=Stirrup-1-lin-1-5-lin-1-5-lin-1-5, generate

1, 44, 1

*Nset, nset=_PickedSet110, internal, instance=Stirrup-1-lin-5-1-lin-1-5-lin-1-9, generate

1, 44, 1

*Nset, nset=_PickedSet110, internal, instance=Stirrup-1-lin-5-5, generate

1, 44, 1

*Nset, nset=_PickedSet110, internal, instance=Stirrup-1-lin-5-1-lin-1-5, generate

1, 44, 1

*Nset, nset=_PickedSet110, internal, instance=Rebar-1-lin-2-1, generate

1, 151, 1

*Nset, nset=_PickedSet110, internal, instance=Stirrup-1-lin-1-4, generate

1, 44, 1

*Nset, nset=_PickedSet110, internal, instance=Stirrup-1-lin-3-2, generate

1, 44, 1

*Nset, nset=_PickedSet110, internal, instance=Stirrup-1-lin-1-5-lin-1-4, generate

1, 44, 1

*Nset, nset=_PickedSet110, internal, instance=Stirrup-1-lin-5-1-lin-1-5-lin-1-4, generate

1, 44, 1

*Nset, nset=_PickedSet110, internal, instance=Stirrup-1-lin-4-5, generate

1, 44, 1

*Nset, nset=_PickedSet110, internal, instance=Stirrup-1-lin-1-5-lin-1-5-lin-1-8, generate

1, 44, 1

*Nset, nset=_PickedSet110, internal, instance=Stirrup-1-lin-2-3, generate

1, 44, 1

*Nset, nset=_PickedSet110, internal, instance=Stirrup-1-lin-4-1, generate

1, 44, 1

*Nset, nset=_PickedSet110, internal, instance=Stirrup-1-lin-1-5-lin-1-5-lin-1-4, generate

1, 44, 1

*Nset, nset=_PickedSet110, internal, instance=Stirrup-1-lin-5-1-lin-1-5-lin-1-8, generate

1, 44, 1

*Nset, nset=_PickedSet110, internal, instance=Stirrup-1-lin-5-4, generate

1, 44, 1

*Nset, nset=_PickedSet110, internal, instance=Stirrup-1-lin-5-1-lin-1-4, generate

1, 44, 1

*Nset, nset=_PickedSet110, internal, instance=Stirrup-1-lin-1-2, generate

1, 44, 1

*Nset, nset=_PickedSet110, internal, instance=Stirrup-1-lin-2-1, generate

1, 44, 1

*Nset, nset=_PickedSet110, internal, instance=Stirrup-1-lin-3-4, generate

1, 44, 1

*Nset, nset=_PickedSet110, internal, instance=Stirrup-1-lin-1-5-lin-1-5-lin-1-2, generate

1, 44, 1

*Nset, nset=_PickedSet110, internal, instance=Stirrup-1-lin-5-1-lin-1-5-lin-1-6, generate

1, 44, 1

*Nset, nset=_PickedSet110, internal, instance=Stirrup-1-lin-5-2, generate

1, 44, 1

*Nset, nset=_PickedSet110, internal, instance=Stirrup-1-lin-5-1-lin-1-2, generate

1, 44, 1

*Nset, nset=_PickedSet110, internal, instance=Stirrup-1-lin-2-5, generate

1, 44, 1

*Nset, nset=_PickedSet110, internal, instance=Stirrup-1-lin-4-3, generate

1, 44, 1

*Nset, nset=_PickedSet110, internal, instance=Stirrup-1-lin-1-5-lin-1-5-lin-1-6, generate

1, 44, 1

*Nset, nset=_PickedSet110, internal, instance=Stirrup-1-lin-1-5-lin-1-2, generate

1, 44, 1

*Nset, nset=_PickedSet110, internal, instance=Stirrup-1-lin-5-1-lin-1-5-lin-1-2, generate

1, 44, 1

*Elset, elset=_PickedSet110, internal, instance=Rebar-1, generate

1, 150, 1

*Elset, elset=_PickedSet110, internal, instance=Stirrup-1, generate

1, 44, 1

*Elset, elset=_PickedSet110, internal, instance=Rebar-1-lin-1-2, generate

1, 150, 1

*Elset, elset=_PickedSet110, internal, instance=Stirrup-1-lin-1-3, generate

1, 44, 1

*Elset, elset=_PickedSet110, internal, instance=Stirrup-1-lin-3-1, generate

1, 44, 1

*Elset, elset=_PickedSet110, internal, instance=Stirrup-1-lin-1-5-lin-1-3, generate

1, 44, 1

*Elset, elset=_PickedSet110, internal, instance=Stirrup-1-lin-5-1-lin-1-5-lin-1-3, generate

1, 44, 1

*Elset, elset=_PickedSet110, internal, instance=Stirrup-1-lin-4-4, generate

1, 44, 1

*Elset, elset=_PickedSet110, internal, instance=Stirrup-1-lin-1-5-lin-1-5-lin-1-7, generate

1, 44, 1

*Elset, elset=_PickedSet110, internal, instance=Stirrup-1-lin-2-2, generate

1, 44, 1

*Elset, elset=_PickedSet110, internal, instance=Stirrup-1-lin-3-5, generate

1, 44, 1

*Elset, elset=_PickedSet110, internal, instance=Stirrup-1-lin-1-5-lin-1-5-lin-1-3, generate

1, 44, 1

*Elset, elset=_PickedSet110, internal, instance=Stirrup-1-lin-5-1-lin-1-5-lin-1-7, generate

1, 44, 1

*Elset, elset=_PickedSet110, internal, instance=Stirrup-1-lin-5-3, generate

1, 44, 1

*Elset, elset=_PickedSet110, internal, instance=Stirrup-1-lin-5-1-lin-1-3, generate

1, 44, 1

*Elset, elset=_PickedSet110, internal, instance=Rebar-1-lin-2-2, generate

1, 150, 1

*Elset, elset=_PickedSet110, internal, instance=Stirrup-1-lin-1-5, generate

1, 44, 1

*Elset, elset=_PickedSet110, internal, instance=Stirrup-1-lin-3-3, generate

1, 44, 1

*Elset, elset=_PickedSet110, internal, instance=Stirrup-1-lin-1-5-lin-1-5, generate

1, 44, 1

*Elset, elset=_PickedSet110, internal, instance=Stirrup-1-lin-5-1-lin-1-5-lin-1-5, generate

1, 44, 1

*Elset, elset=_PickedSet110, internal, instance=Stirrup-1-lin-5-1, generate

1, 44, 1

*Elset, elset=_PickedSet110, internal, instance=Stirrup-1-lin-1-5-lin-1-5-lin-1-9, generate

1, 44, 1

*Elset, elset=_PickedSet110, internal, instance=Stirrup-1-lin-2-4, generate

1, 44, 1

*Elset, elset=_PickedSet110, internal, instance=Stirrup-1-lin-4-2, generate

1, 44, 1

*Elset, elset=_PickedSet110, internal, instance=Stirrup-1-lin-1-5-lin-1-5-lin-1-5, generate

1, 44, 1

*Elset, elset=_PickedSet110, internal, instance=Stirrup-1-lin-5-1-lin-1-5-lin-1-9, generate

1, 44, 1

*Elset, elset=_PickedSet110, internal, instance=Stirrup-1-lin-5-5, generate

1, 44, 1

*Elset, elset=_PickedSet110, internal, instance=Stirrup-1-lin-5-1-lin-1-5, generate

1, 44, 1

*Elset, elset=_PickedSet110, internal, instance=Rebar-1-lin-2-1, generate

1, 150, 1

*Elset, elset=_PickedSet110, internal, instance=Stirrup-1-lin-1-4, generate

1, 44, 1

*Elset, elset=_PickedSet110, internal, instance=Stirrup-1-lin-3-2, generate

1, 44, 1

*Elset, elset=_PickedSet110, internal, instance=Stirrup-1-lin-1-5-lin-1-4, generate

1, 44, 1

*Elset, elset=_PickedSet110, internal, instance=Stirrup-1-lin-5-1-lin-1-5-lin-1-4, generate

1, 44, 1

*Elset, elset=_PickedSet110, internal, instance=Stirrup-1-lin-4-5, generate

1, 44, 1

*Elset, elset=_PickedSet110, internal, instance=Stirrup-1-lin-1-5-lin-1-5-lin-1-8, generate

1, 44, 1

*Elset, elset=_PickedSet110, internal, instance=Stirrup-1-lin-2-3, generate

1, 44, 1

*Elset, elset=_PickedSet110, internal, instance=Stirrup-1-lin-4-1, generate

1, 44, 1

*Elset, elset=_PickedSet110, internal, instance=Stirrup-1-lin-1-5-lin-1-5-lin-1-4, generate

1, 44, 1

*Elset, elset=_PickedSet110, internal, instance=Stirrup-1-lin-5-1-lin-1-5-lin-1-8, generate

1, 44, 1

*Elset, elset=_PickedSet110, internal, instance=Stirrup-1-lin-5-4, generate

1, 44, 1

*Elset, elset=_PickedSet110, internal, instance=Stirrup-1-lin-5-1-lin-1-4, generate

1, 44, 1

*Elset, elset=_PickedSet110, internal, instance=Stirrup-1-lin-1-2, generate

1, 44, 1

*Elset, elset=_PickedSet110, internal, instance=Stirrup-1-lin-2-1, generate

1, 44, 1

*Elset, elset=_PickedSet110, internal, instance=Stirrup-1-lin-3-4, generate

1, 44, 1

*Elset, elset=_PickedSet110, internal, instance=Stirrup-1-lin-1-5-lin-1-5-lin-1-2, generate

1, 44, 1

*Elset, elset=_PickedSet110, internal, instance=Stirrup-1-lin-5-1-lin-1-5-lin-1-6, generate

1, 44, 1

*Elset, elset=_PickedSet110, internal, instance=Stirrup-1-lin-5-2, generate

1, 44, 1

*Elset, elset=_PickedSet110, internal, instance=Stirrup-1-lin-5-1-lin-1-2, generate

1, 44, 1

*Elset, elset=_PickedSet110, internal, instance=Stirrup-1-lin-2-5, generate

1, 44, 1

*Elset, elset=_PickedSet110, internal, instance=Stirrup-1-lin-4-3, generate

1, 44, 1

*Elset, elset=_PickedSet110, internal, instance=Stirrup-1-lin-1-5-lin-1-5-lin-1-6, generate

1, 44, 1

*Elset, elset=_PickedSet110, internal, instance=Stirrup-1-lin-1-5-lin-1-2, generate

1, 44, 1

*Elset, elset=_PickedSet110, internal, instance=Stirrup-1-lin-5-1-lin-1-5-lin-1-2, generate

1, 44, 1

*Nset, nset=_PickedSet111, internal, instance=Concrete-1, generate

1, 38656, 1

*Elset, elset=_PickedSet111, internal, instance=Concrete-1, generate

1, 33750, 1

*Nset, nset=_PickedSet112, internal, instance=Concrete-1

1, 2, 3, 4, 5, 6, 7, 8, 9, 10, 11, 12, 13, 14, 15, 16

2417, 2418, 2419, 2420, 2421, 2422, 2423, 2424, 2425, 2426, 2427, 2428, 2429, 2430, 2431, 2432

4833, 4834, 4835, 4836, 4837, 4838, 4839, 4840, 4841, 4842, 4843, 4844, 4845, 4846, 4847, 4848

7249, 7250, 7251, 7252, 7253, 7254, 7255, 7256, 7257, 7258, 7259, 7260, 7261, 7262, 7263, 7264

9665, 9666, 9667, 9668, 9669, 9670, 9671, 9672, 9673, 9674, 9675, 9676, 9677, 9678, 9679, 9680

12081, 12082, 12083, 12084, 12085, 12086, 12087, 12088, 12089, 12090, 12091, 12092, 12093, 12094, 12095, 12096

14497, 14498, 14499, 14500, 14501, 14502, 14503, 14504, 14505, 14506, 14507, 14508, 14509, 14510, 14511, 14512

16913, 16914, 16915, 16916, 16917, 16918, 16919, 16920, 16921, 16922, 16923, 16924, 16925, 16926, 16927, 16928

19329, 19330, 19331, 19332, 19333, 19334, 19335, 19336, 19337, 19338, 19339, 19340, 19341, 19342, 19343, 19344

21745, 21746, 21747, 21748, 21749, 21750, 21751, 21752, 21753, 21754, 21755, 21756, 21757, 21758, 21759, 21760

24161, 24162, 24163, 24164, 24165, 24166, 24167, 24168, 24169, 24170, 24171, 24172, 24173, 24174, 24175, 24176

26577, 26578, 26579, 26580, 26581, 26582, 26583, 26584, 26585, 26586, 26587, 26588, 26589, 26590, 26591, 26592

28993, 28994, 28995, 28996, 28997, 28998, 28999, 29000, 29001, 29002, 29003, 29004, 29005, 29006, 29007, 29008

31409, 31410, 31411, 31412, 31413, 31414, 31415, 31416, 31417, 31418, 31419, 31420, 31421, 31422, 31423, 31424

33825, 33826, 33827, 33828, 33829, 33830, 33831, 33832, 33833, 33834, 33835, 33836, 33837, 33838, 33839, 33840

36241, 36242, 36243, 36244, 36245, 36246, 36247, 36248, 36249, 36250, 36251, 36252, 36253, 36254, 36255, 36256

*Elset, elset=_PickedSet112, internal, instance=Concrete-1

1, 2, 3, 4, 5, 6, 7, 8, 9, 10, 11, 12, 13, 14, 15, 2251

2252, 2253, 2254, 2255, 2256, 2257, 2258, 2259, 2260, 2261, 2262, 2263, 2264, 2265, 4501, 4502

4503, 4504, 4505, 4506, 4507, 4508, 4509, 4510, 4511, 4512, 4513, 4514, 4515, 6751, 6752, 6753

6754, 6755, 6756, 6757, 6758, 6759, 6760, 6761, 6762, 6763, 6764, 6765, 9001, 9002, 9003, 9004

9005, 9006, 9007, 9008, 9009, 9010, 9011, 9012, 9013, 9014, 9015, 11251, 11252, 11253, 11254, 11255

11256, 11257, 11258, 11259, 11260, 11261, 11262, 11263, 11264, 11265, 13501, 13502, 13503, 13504, 13505, 13506

13507, 13508, 13509, 13510, 13511, 13512, 13513, 13514, 13515, 15751, 15752, 15753, 15754, 15755, 15756, 15757

15758, 15759, 15760, 15761, 15762, 15763, 15764, 15765, 18001, 18002, 18003, 18004, 18005, 18006, 18007, 18008

18009, 18010, 18011, 18012, 18013, 18014, 18015, 20251, 20252, 20253, 20254, 20255, 20256, 20257, 20258, 20259

20260, 20261, 20262, 20263, 20264, 20265, 22501, 22502, 22503, 22504, 22505, 22506, 22507, 22508, 22509, 22510

22511, 22512, 22513, 22514, 22515, 24751, 24752, 24753, 24754, 24755, 24756, 24757, 24758, 24759, 24760, 24761

24762, 24763, 24764, 24765, 27001, 27002, 27003, 27004, 27005, 27006, 27007, 27008, 27009, 27010, 27011, 27012

27013, 27014, 27015, 29251, 29252, 29253, 29254, 29255, 29256, 29257, 29258, 29259, 29260, 29261, 29262, 29263

29264, 29265, 31501, 31502, 31503, 31504, 31505, 31506, 31507, 31508, 31509, 31510, 31511, 31512, 31513, 31514

31515,

*Nset, nset=_PickedSet113, internal, instance=Concrete-1

2401, 2402, 2403, 2404, 2405, 2406, 2407, 2408, 2409, 2410, 2411, 2412, 2413, 2414, 2415, 2416

4817, 4818, 4819, 4820, 4821, 4822, 4823, 4824, 4825, 4826, 4827, 4828, 4829, 4830, 4831, 4832

7233, 7234, 7235, 7236, 7237, 7238, 7239, 7240, 7241, 7242, 7243, 7244, 7245, 7246, 7247, 7248

9649, 9650, 9651, 9652, 9653, 9654, 9655, 9656, 9657, 9658, 9659, 9660, 9661, 9662, 9663, 9664

12065, 12066, 12067, 12068, 12069, 12070, 12071, 12072, 12073, 12074, 12075, 12076, 12077, 12078, 12079, 12080

14481, 14482, 14483, 14484, 14485, 14486, 14487, 14488, 14489, 14490, 14491, 14492, 14493, 14494, 14495, 14496

16897, 16898, 16899, 16900, 16901, 16902, 16903, 16904, 16905, 16906, 16907, 16908, 16909, 16910, 16911, 16912

19313, 19314, 19315, 19316, 19317, 19318, 19319, 19320, 19321, 19322, 19323, 19324, 19325, 19326, 19327, 19328

21729, 21730, 21731, 21732, 21733, 21734, 21735, 21736, 21737, 21738, 21739, 21740, 21741, 21742, 21743, 21744

24145, 24146, 24147, 24148, 24149, 24150, 24151, 24152, 24153, 24154, 24155, 24156, 24157, 24158, 24159, 24160

26561, 26562, 26563, 26564, 26565, 26566, 26567, 26568, 26569, 26570, 26571, 26572, 26573, 26574, 26575, 26576

28977, 28978, 28979, 28980, 28981, 28982, 28983, 28984, 28985, 28986, 28987, 28988, 28989, 28990, 28991, 28992

31393, 31394, 31395, 31396, 31397, 31398, 31399, 31400, 31401, 31402, 31403, 31404, 31405, 31406, 31407, 31408

33809, 33810, 33811, 33812, 33813, 33814, 33815, 33816, 33817, 33818, 33819, 33820, 33821, 33822, 33823, 33824

36225, 36226, 36227, 36228, 36229, 36230, 36231, 36232, 36233, 36234, 36235, 36236, 36237, 36238, 36239, 36240

38641, 38642, 38643, 38644, 38645, 38646, 38647, 38648, 38649, 38650, 38651, 38652, 38653, 38654, 38655, 38656

*Elset, elset=_PickedSet113, internal, instance=Concrete-1

2236, 2237, 2238, 2239, 2240, 2241, 2242, 2243, 2244, 2245, 2246, 2247, 2248, 2249, 2250, 4486

4487, 4488, 4489, 4490, 4491, 4492, 4493, 4494, 4495, 4496, 4497, 4498, 4499, 4500, 6736, 6737

6738, 6739, 6740, 6741, 6742, 6743, 6744, 6745, 6746, 6747, 6748, 6749, 6750, 8986, 8987, 8988

8989, 8990, 8991, 8992, 8993, 8994, 8995, 8996, 8997, 8998, 8999, 9000, 11236, 11237, 11238, 11239

11240, 11241, 11242, 11243, 11244, 11245, 11246, 11247, 11248, 11249, 11250, 13486, 13487, 13488, 13489, 13490

13491, 13492, 13493, 13494, 13495, 13496, 13497, 13498, 13499, 13500, 15736, 15737, 15738, 15739, 15740, 15741

15742, 15743, 15744, 15745, 15746, 15747, 15748, 15749, 15750, 17986, 17987, 17988, 17989, 17990, 17991, 17992

17993, 17994, 17995, 17996, 17997, 17998, 17999, 18000, 20236, 20237, 20238, 20239, 20240, 20241, 20242, 20243

20244, 20245, 20246, 20247, 20248, 20249, 20250, 22486, 22487, 22488, 22489, 22490, 22491, 22492, 22493, 22494

22495, 22496, 22497, 22498, 22499, 22500, 24736, 24737, 24738, 24739, 24740, 24741, 24742, 24743, 24744, 24745

24746, 24747, 24748, 24749, 24750, 26986, 26987, 26988, 26989, 26990, 26991, 26992, 26993, 26994, 26995, 26996

26997, 26998, 26999, 27000, 29236, 29237, 29238, 29239, 29240, 29241, 29242, 29243, 29244, 29245, 29246, 29247

29248, 29249, 29250, 31486, 31487, 31488, 31489, 31490, 31491, 31492, 31493, 31494, 31495, 31496, 31497, 31498

31499, 31500, 33736, 33737, 33738, 33739, 33740, 33741, 33742, 33743, 33744, 33745, 33746, 33747, 33748, 33749

33750,

*Elset, elset=__PickedSurf114_S1, internal, instance=Concrete-1, generate

31501, 33750, 1

*Surface, type=ELEMENT, name=_PickedSurf114, internal

__PickedSurf114_S1, S1

** Constraint: Embedded

*Embedded Element, host elset=_PickedSet111

_PickedSet110

*End Assembly

*Amplitude, name=Amp-1

0., 30., 0.001624, 0.

**

```
** MATERIALS
**
*Material, name=C-41
*Density
 2.4e-09,
*Elastic
35000., 0.2
*Concrete Damaged Plasticity
31.,   0.1,  1.16, 0.667,    0.
*Concrete Compression Hardening
 12.8379,          0.,        0.05
 22.6172, 0.000150766,        0.05
 29.4079, 0.000368223,        0.05
 33.2778, 0.000677529,        0.05
  34.32,  0.00101544,         0.05
 34.2926,  0.00107662,        0.05
 32.5163,  0.00156348,        0.05
 28.0107,  0.00213616,        0.05
  20.836,  0.00279278,        0.05
 19.7928,  0.00287759,        0.05
*Concrete Tension Stiffening,
type=DISPLACEMENT
   2.65447,      0.,    0.05
   2.2457,    0.01,    0.05
  1.83693,    0.02,    0.05
  1.42815,    0.03,    0.05
  1.01938,    0.04,    0.05
 0.610607,    0.05,    0.05
0.530895, 0.05195,    0.05
 0.510328,    0.06,    0.05
  0.48478,    0.07,    0.05
 0.459232,    0.08,    0.05
 0.433683,    0.09,    0.05
 0.408135,     0.1,    0.05
 0.382587,    0.11,    0.05
 0.357038,    0.12,    0.05
  0.33149,    0.13,    0.05
 0.305942,    0.14,    0.05
 0.280393,    0.15,    0.05
 0.254845,    0.16,    0.05
 0.229297,    0.17,    0.05
 0.203748,    0.18,    0.05
   0.1782,    0.19,    0.05
 0.152652,     0.2,    0.05
 0.127103,    0.21,    0.05
 0.101555,    0.22,    0.05
```

0.0760066, 0.23, 0.05

0.0504583, 0.24, 0.05

0.0249099, 0.25, 0.05

*Concrete Compression Damage

0., 0.

0., 0.000150766

0., 0.000368223

0., 0.000677529

0., 0.00101544

0.000798117, 0.00107662

0.0525563, 0.00156348

0.183837, 0.00213616

0.39289, 0.00279278

0.423288, 0.00287759

*Concrete Tension Damage

0., 0.

0.153994, 0.01

0.307988, 0.02

0.461982, 0.03

0.615977, 0.04

0.769971, 0.05

0.8, 0.05195

0.807748, 0.06

0.817372, 0.07

0.826997, 0.08

0.836622, 0.09

0.846246, 0.1

0.855871, 0.11

0.865496, 0.12

0.87512, 0.13

0.884745, 0.14

0.89437, 0.15

0.903994, 0.16

0.913619, 0.17

0.923243, 0.18

0.932868, 0.19

0.942493, 0.2

0.952117, 0.21

0.961742, 0.22

0.971367, 0.23

0.980991, 0.24

0.990616, 0.25

*Material, name=Steel

*Density

7.85e-09,

*Elastic

```
210000., 0.3
*Plastic
400.,0.
**
** BOUNDARY CONDITIONS
**
** Name: Bottom Fixed Type: Symmetry/Antisymmetry/Encastre
*Boundary
_PickedSet112, ENCASTRE
** Name: Top Fixed Type: Symmetry/Antisymmetry/Encastre
*Boundary
_PickedSet113, ENCASTRE
** ----------------------------------------------
**
** STEP: Blast Load
**
*Step, name="Blast Load", nlgeom=YES
*Dynamic, Explicit
, 0.001624
*Bulk Viscosity
0.06, 1.2
**
** LOADS
**
** Name: Blast Loading   Type: Pressure
*Dsload, amplitude=Amp-1
_PickedSurf114, P, 1.
**
** OUTPUT REQUESTS
**
*Restart, write, number interval=1, time marks=NO
**
** FIELD OUTPUT: F-Output-1
**
*Output, field
*Node Output
A, RF, U, V
*Element Output, directions=YES
DAMAGEC, DAMAGET, LE, PE, PEEQ, S
**
** HISTORY OUTPUT: H-Output-1
*Output, history, variable=PRESELECT
*End Step
```